

# GeXSe (Generative Explanatory Sensor System): An Interpretable Deep Generative Model for Human Activity Recognition in Smart Spaces

YUAN SUN, Rutgers, The State University of New Jersey, .  
 NANDANA PAI, Rutgers, The State University of New Jersey, .  
 VISWA VIJETH RAMESH, Rutgers, The State University of New Jersey, .  
 MURTADHA ALDEER, Rutgers, The State University of New Jersey, .  
 JORGE ORTIZ, Rutgers, The State University of New Jersey, .

We introduce GeXSe (Generative Explanatory Sensor System), a novel framework designed to extract interpretable sensor-based and vision domain features from non-invasive smart space sensors. We combine these to provide a comprehensive explanation of sensor-activation patterns in activity recognition tasks. This system leverages advanced machine learning architectures, including transformer blocks, Fast Fourier Convolution (FFC), and diffusion models, to provide a more detailed understanding of sensor-based human activity data. A standout feature of GeXSe is our unique Multi-Layer Perceptron (MLP) with linear, ReLU, and normalization layers, specially devised for optimal performance on small datasets. It also yields meaningful activation maps to explain sensor-based activation patterns. The standard approach is based on a CNN model, which our MLP model outperforms. GeXSe offers two types of explanations: sensor-based activation maps and visual domain explanations using short videos. These methods offer a comprehensive interpretation of the output from non-interpretable sensor data, thereby augmenting the interpretability of our model. Utilizing the Frechet Inception Distance (FID) for evaluation, it outperforms established methods, improving baseline performance by about 6%. GeXSe also achieves a high F1 score of up to 0.85, demonstrating precision, recall, and noise resistance, marking significant progress in reliable and explainable smart space sensing systems.

CCS Concepts: • **Computing methodologies** → **Machine learning**; • **Human-centered computing** → **Visualization**.

Additional Key Words and Phrases: Explainable IoT, Deep generative model, Hardware deep learning, Deep learning on small dataset

## ACM Reference Format:

Yuan Sun, Nandana Pai, Viswa Vijeth Ramesh, Murtadha Aldeer, and Jorge Ortiz. 2023. GeXSe (Generative Explanatory Sensor System): An Interpretable Deep Generative Model for Human Activity Recognition in Smart Spaces. . 0, 0, Article 0 (2023), 35 pages. <https://doi.org/10.1145/nnnnnnn.nnnnnnn>

## 1 INTRODUCTION

Recently, there has been an overwhelming influx of sensor devices and smart home solutions from established and emerging brands. These innovative offerings aim to address various daily-life challenges, such as convenience, energy efficiency, security, and automation. From smart home hubs to motion detectors and smart kitchen appliances, these devices provide centralized control, remote monitoring and control capabilities, motion detection, energy optimization, and enhanced convenience in different aspects of our daily lives [20, 34]. The field of ubiquitous and pervasive computing envisions a future where personalized interactions between individuals and

<sup>1</sup>This study was approved by the Institutional Review Board at our institution (IRB No. \_\_\_\_\_)

Authors' addresses: Yuan Sun, Rutgers, The State University of New Jersey, ., ys820@rutgers.edu; Nandana Pai, Rutgers, The State University of New Jersey, ., np761@scarletmail.rutgers.edu; Viswa Vijeth Ramesh, Rutgers, The State University of New Jersey, ., viswavijeth.ramesh@rutgers.edu; Murtadha Aldeer, Rutgers, The State University of New Jersey, ., maldeer@winlab.rutgers.edu; Jorge Ortiz, Rutgers, The State University of New Jersey, ., jorge.ortiz@rutgers.edu.

2023. 2474-9567/2023/0-ART0 \$0.00  
<https://doi.org/10.1145/nnnnnnn.nnnnnnn>

their environment are seamlessly integrated. However, the realization of this vision is impeded by the lack of a clear roadmap for transitioning from concept to widespread implementation. While prototypes of sensors and actuators have been developed to capture real-world information and offer novel functionalities, there is a need for a comprehensive framework that transforms these devices into an interconnected and intelligent computing system that can seamlessly adapt to users' environments [38].

Smart space sensor-based human activity recognition (HAR) has attracted significant research interest in the field of ubiquitous computing. Various solutions have been proposed, primarily focusing on sensor-based recognition methods [29]. While traditional machine learning approaches, such as rule-based and statistical methods, have achieved notable success in HAR [25], they still suffer from inherent limitations. These limitations include the need for handcrafted features, the difficulty in capturing complex temporal dependencies, challenges in handling large-scale datasets, and the necessity of addressing issues related to parameter sharing between deep and shallow models [137]. In recent years, deep learning techniques have emerged as a superior approach for HAR. These techniques, with their ability to automatically learn features and model complex relationships, have shown great promise in overcoming the limitations of traditional approaches, leading to extensive research in applying deep learning to the field of activity recognition [48, 93].

Deep learning-based interpretation of sensor features has predominantly focused on semantic explanation [10, 14, 64, 71, 106, 113, 146]. However, there is a notable scarcity of research dedicated to developing a comprehensive representation of features in the vision domain [58]. This represents an untapped potential for generating interpretable features within sensor-based deep-learning models. As smart space systems generate spatiotemporally co-occurring sensor streams from diverse sources, there is a growing need to enable these systems to effectively interpret and derive meaningful insights from their data. Exploring the use of deep generative models holds great promise in delivering human-understandable features within the domain of smart space sensors, bridging the gap between advanced analytics and interpretability.

Privacy and cost concerns surrounding camera-based surveillance in smart homes have shifted the focus towards non-intrusive sensors as a viable alternative [27, 129]. Ambient sensing systems have emerged as an exciting area of research, offering low-cost, non-intrusive, and privacy-preserving solutions [16, 28, 68, 85, 132, 140, 143]. These systems leverage various sensors and techniques to collect environmental information such as temperature, humidity, sound, and vibration. By creating an interconnected network of everyday objects, real-time communication and inference of activities in space become possible, providing continuous event logs and enabling the derivation of novel synthetic sensors with enhanced semantic richness [81].

However, extracting explainable features from non-camera-based sensor data poses significant challenges [9]. Distribution shifts driven by external factors, including the physical space, sensor placement, and type, distance to activities, activity types, and event co-occurrence, complicate the generation of interpretable representations. While research in ambient sensing has made progress in developing sophisticated models, many of these models still exhibit limitations when mapping features to pre-specified label spaces, restricting their expressivity and interpretability, especially in cases of ambiguous activities [139]. Nevertheless, the exploration of explainable features in non-camera-based ambient sensing systems continues to drive innovation and holds promise in bridging the gap between raw sensor data and human-understandable insights.

In this paper, we propose a novel approach that establishes a correlation between sensors in smart spaces and the extraction of visual features in the vision domain. To create a system capable of such feature extraction and interpretation, we have employed a Fast Fourier Convolution (FFC) in the encoder and both an FCC and a state-of-the-art transformer block in the design of our decoder. These components are crucial in handling the time-series sensor data effectively, allowing for a thorough and accurate analysis. Furthermore, our decoder integrates a diffusion model to facilitate the generation of vision domain explanations. This unique combination of technologies forms the backbone of GeXSe, enabling it to provide detailed and understandable insights into sensor and visual domain data.

Unlike existing CNN-based methods for generating explainable features, we develop our own encoder specifically tailored to a small dataset. Our encoder produces features at the sensor level, offering a transparent and understandable representation of the data. Furthermore, we extend our approach by incorporating a decoder to explore visual domain explanations. This unique capability enables users, even those without a machine learning background, to effortlessly comprehend both analysis and explanations at the sensor level and in the visual domain. To validate the effectiveness of our approach, we conduct comprehensive experiments on two distinct datasets. The first dataset is collected using our custom-built device, which addresses important concerns associated with non-intrusive sensors. The second dataset is a well-known public dataset, serving as evidence of the generalizability of our approach, referred to as GeXSe (Generative Explanatory Sensor System). Our experimental results demonstrate the feasibility of extracting interpretable visual features associated with activities in physical space using measurements obtained from ambient, non-intrusive sensors. By introducing GeXSe and showcasing its capabilities in extracting meaningful visual features, this work contributes to the advancement of explainable sensing systems. The transparency and interpretability offered by our approach provide valuable insights for various applications in smart spaces, promoting user understanding and trust. Importantly, our model demonstrated a significant performance improvement, achieving a gain of approximately 6.55 units over the lower layer activation map and about 3.82 units over the higher layer activation map in the FID metric. Furthermore, GeXSe has impressively achieved an F1 score of up to 0.85, underscoring its effectiveness in smart-space activity recognition.

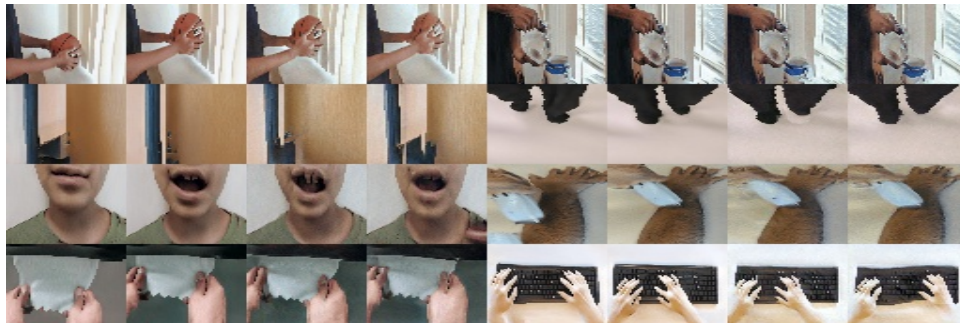


Fig. 1. Video generated from the ambient sensors and no camera. The activities detected by sensors are playing basketball, door passing, eating, pulling a paper, pouring water, running, shaving, and typing. Different frames show movements in each video.

Recent research has primarily focused on utilizing natural language processing (NLP) models to extract semantic features from sensor data. However, there exists a significant research gap in generating highly interpretable features (see Figure 2), that provide insights into both the sensor and vision domains within the context of smart space sensors (see Figure 1). A key strength of GeXSe lies in its robustness against noise and its adaptability to various sensor types and changes in data collection methods. This resilience to noise and adaptability makes GeXSe a versatile solution suitable for a wide range of smart space environments, accommodating diverse sensing technologies and data conditions. Such versatility ensures GeXSe's effectiveness in the face of evolving smart space technologies and varied use cases, thereby bridging the existing research gap.

To address this gap, our work makes several noteworthy contributions:

- We introduce a novel framework that enables the extraction of explainable features from ambient sensor measurements, encompassing both the sensor and vision domains.

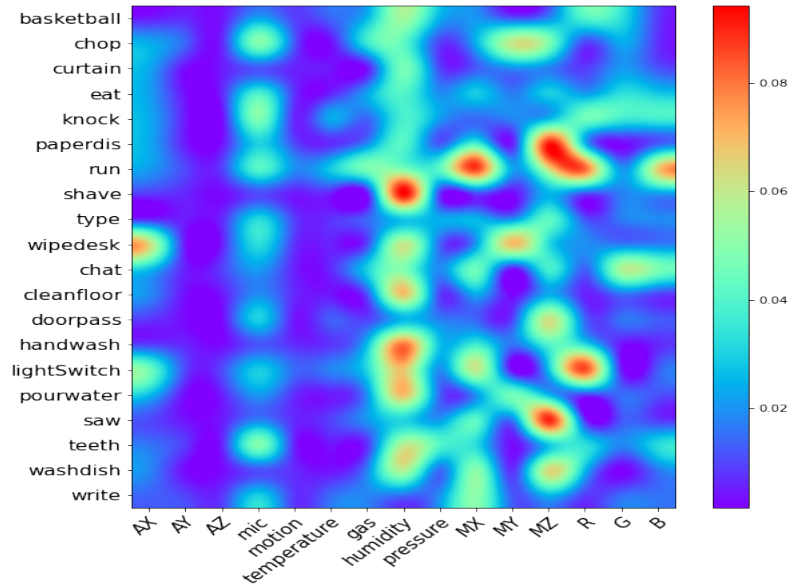


Fig. 2. We design the gradient-based sensor activation map using our unique MLP design, specially designed to work with small data sets. This is a departure from the typical CNN structure, which does not perform well in the aforementioned small-data case.

- We design an optimized encoder specifically tailored for small-sized datasets, allowing for effective feature capture and providing insightful explanations through the use of *sensor-based activation maps* that highlight the importance of different sensor and visual elements.
- We develop a decoder based on advanced deep generative models, enhancing its performance in generating clear and interpretable explanations in the visual domain.
- We conduct extensive experiments on both proprietary and publicly available datasets to demonstrate the generalizability and effectiveness of our approach in generating meaningful *activation maps* and interpretable explanations.
- We ensure that the explanations provided by our model are accessible and comprehensible to users without a background in machine learning, empowering them to understand the underlying sensor and vision domain features through the visualization of *activation maps*.

In the subsequent sections of this paper, we discuss related work, provide an overview of our proposed methodology, present the experimental results, and offer a thorough analysis of the implications of our model, along with potential avenues for future research.

## 2 RELATED WORK

### 2.1 Activity Sensing in Spaces

**2.1.1 Camera-based HAR.** The camera has found extensive utilization in computer vision for Human Activity Recognition (HAR) [41, 56, 105, 145], with numerous significant applications such as human-computer interfaces,

content-based video indexing, video surveillance, and robotics, among others. Cameras offer plentiful indirect data that can be processed using methods such as machine learning to produce sensor-like data streams. Additionally, cameras are presently accessible at budget-friendly prices, and their costs are steadily approaching a significantly affordable level [42, 81].

However, ensuring accessibility to physical interfaces has posed an enduring challenge [43, 97], as certain actions cannot be performed solely through cameras. For instance, the ability to turn on or off a light switch typically requires direct physical interaction. Similarly, tasks such as adjusting volume knobs or pressing physical buttons on devices cannot be accomplished through camera-based methods alone. Thus, while cameras provide valuable input for various applications, there are still limitations when it comes to directly controlling physical objects or interfaces. Although developing new accessible devices is a potential solution, it is unlikely to be implemented across all devices due to cost considerations.

The integration of *general-purpose sensing* may gradually address this issue. As more devices become interconnected and capable of remote control, the challenge shifts towards digital accessibility, which is comparatively easier to resolve. This shift allows for the implementation of digital solutions to enhance accessibility, making it more feasible to provide inclusive access to a wide range of devices [49].

Additionally, privacy and cost highly limit the broad-scale deployment of cameras. Several studies focus on its social intrusiveness [15, 22, 37, 57]. This concern makes the camera impossible to generalize to all occasions. As a result, general-purpose sensing can not take a camera as part of its sensor. Moreover, some signals can not be detected by cameras [111]. The most recent successful sensor company developed devices that can detect human activities, earthquakes, and other signals that can not be directly monitored by cameras at home [112]. Much of the current research is also based on these types of sensors [26, 55, 89, 133, 138].

**2.1.2 General-Purpose Sensing.** The concept of general-purpose sensing involves the capacity to detect various activities within a smart environment utilizing either a single sensor within that space or a minimal deployment spread across numerous or expansive spaces. Sensor boards are increasingly equipped with diverse underlying sensors, enabling versatile applications. These boards can be considered general-purpose due to their ability to be attached to various objects and sense multiple aspects without requiring modifications. This approach aligns more closely with a distributed sensing system that facilitates many-to-many interactions [81]. General-purpose sensing differs from conventional approaches by avoiding hardware-level modifications. It encompasses two distinct levels: device level and server level. At the device level, sensor tags are assembled, capable of capturing data from multiple sensing dimensions, which encompass the desired physical sensors. The collected low-level data is then transmitted to the server level. On the server level, machine learning algorithms are employed to process this raw data, transforming it into valuable insights for users. Essentially, general-purpose sensing establishes a platform that encompasses all necessary raw data types and extends its capabilities through server-based machine learning analytics [147].

As a recently established field, few studies have investigated the efficacy of deep learning algorithms in analyzing data streams from such systems. However, it is important to note that deep learning, in combination with deep explanation methods, has the unique potential to develop meaningful and explainable features for numerous occasions in daily life. In this paper, we explore and demonstrate both properties and demonstrate that high-level semantic information can be generated from simple physical measurement streams.

Based on the aforementioned works, we build our sensor to further explore the generalization of such work. We adjust some parts for sensor-wise explainability. we process the data collected by these sensors. The ubiquitous of these types of sensors can additionally prove the value of our model for ubiquitous computing for smart space.

## 2.2 Context Perception

A context-aware system in a smart home environment is essential for anticipating and fulfilling the needs of users by leveraging their contextual information. The primary objective of a smart home is to predict user demands and deliver appropriate services proactively. By considering the user's context, such systems aim to maximize user comfort and safety while minimizing their explicit interaction with the home environment [66]. In order to establish a context, it is crucial to describe the information originating from that context. This requires the context-awareness system to be supplied with contextual data that possess a semantic level of understanding. These contextual details embody the environment and are perceived within it. Perception, in the context of *sensor* usage, revolves around quantifying physical phenomena. Sensors play a crucial role in capturing activities stemming from the inhabitant's environment within the smart home. By employing heterogeneous *sensors*, the context perception architecture acquires contextual information relevant to both the inhabitant and their surroundings. This approach ensures the provision of meaningful contextual insights through effective sensor-based perception [120].

**2.2.1 Conventional context perception method.** Smart space sensors offer abundant ambient information that proves invaluable for context perception. For instance, temperature sensors enable the monitoring of room climate, motion sensors detect human presence, and light sensors provide information about ambient lighting conditions. Such sensor-based techniques have greatly contributed to enhancing the understanding of contextual factors in smart spaces.

Despite notable advancements, human activity recognition continues to pose challenges as it encompasses a wide array of activities and exhibits diverse variations in their execution. The utilization of machine learning that effectively distinguishes between different activities holds paramount importance in addressing this challenge. Traditional machine learning methods relying on sensors have made significant advancements in perceiving the context within smart spaces [25, 82]. These approaches leverage various sensing technologies to gain insights into the surrounding environment [13, 19, 33, 59, 135]. These conventional methods heavily depend on feature extraction techniques such as time-frequency transformations [60], statistical approaches [24], and symbolic representation [84]. However, the features extracted from these techniques are often meticulously crafted and heuristic in nature. There is a lack of universally applicable or systematic feature extraction approaches that can effectively capture distinct features for human activities.

Traditional methods for activity recognition in human activity recognition (HAR) suffer from various limitations that are effectively addressed by deep learning techniques. Initially, these approaches heavily rely on manually designed and rule-based feature extraction, which restricts their adaptability across diverse environments and tasks. Furthermore, they typically focus on raw data features that can only identify basic activities, thereby posing challenges in inferring complex or contextually-aware activities. Another drawback of conventional HAR approaches is their reliance on large labeled datasets for training, which are often unavailable in practical scenarios. Moreover, most traditional HAR models primarily learn from static data, while real-world activity data is dynamic, necessitating robust online and incremental learning methods [137]. Hence, deep learning emerges as an optimal approach for activity recognition (HAR) and has been extensively investigated in previous studies [4, 79, 107].

**2.2.2 Advanced context perception method.** With its origins in conventional machine learning, deep learning surpasses its predecessors by a wide margin. It employs graph-based methodologies and neuron transformations to construct multi-layered learning models. Numerous cutting-edge deep learning techniques have been introduced, showcasing impressive outcomes across diverse application domains [108]. Deep learning algorithms possess the ability to automate feature extraction, allowing researchers to extract discriminative features with minimal dependence on domain expertise and human intervention [99]. These algorithms employ a hierarchical structure

of data representation, wherein the upper layers of the networks capture high-level features, while the lower layers extract low-level features. Various deep-learning techniques have been employed within the realm of sensor-based applications.

Collecting smart space sensor data is challenging due to privacy concerns, installation and maintenance efforts, user acceptance, and data accessibility. Privacy concerns lead to restricted or anonymized data collection, resulting in smaller datasets. Installation and maintenance of sensors are time-consuming and costly, limiting the number of sensors and data collected. User acceptance may be hindered by privacy and monitoring concerns. Additionally, data accessibility and ownership issues restrict access to smart space sensor data. These factors contribute to the limited availability and small size of smart space sensor data. Hence, a significant unresolved obstacle in this domain pertains to the scarcity of training data [123].

In this study, we conducted experiments to tackle this concern by focusing on the design of our sensor encoder.

### 2.3 Explainable AI

Individuals without a background in machine learning cannot depend on opaque methods for their strategies, as the impartial process of analyzing non-linear signals cannot be elucidated using current advanced frameworks or fundamental statistical analysis [126]. In smart sensing systems, it is particularly common for real-life application users to lack familiarity with deep learning techniques. For example, research studies have explicitly highlighted the "significant limitation" of AI in dermatology due to its inherent black-box nature, which prevents it from conducting personalized evaluations akin to those performed by qualified dermatologists. Such evaluations are crucial for elucidating clinical details and establishing accurate diagnoses [46]. However, within the medical domain, the matter of interpretability extends well beyond theoretical advancements. Specifically, it is observed that interpretability in clinical sectors encompasses unique considerations that are not acknowledged in other fields. These considerations encompass factors such as risk assessment and the associated responsibilities [36, 104].

In recent times, considerable efforts have been directed toward resolving the aforementioned problem of limited comprehension surrounding AI-based systems, including their reasoning processes and outputs. The field of explainable AI (XAI) has emerged as a key research area that actively invests substantial resources to address this issue [6, 75, 80, 103]. Nevertheless, comprehending certain aspects of a system serves as a transitional phase towards achieving broader objectives [6, 80, 98]. Through comprehending the process by which a specific system generates its outputs, such as identifying which sensor is activated in a particular situation, individuals gain the ability to evaluate whether the output is derived from valid criteria or not [103, 127].

**2.3.1 Transparent model.** To attain intrinsic interpretability, one can develop self-explanatory models that integrate interpretability directly into their structures. These purposely designed interpretable models possess the capability to offer explanations either on a global scale or on an individual prediction basis. Several traditional machine learning algorithms, such as Linear/Logistic regression, Decision trees, K-Nearest Neighbors (KNN), Rule-based learning, General additive models (GAM), and Bayesian models, fall into this category of models. Linear/Logistic regression models offer transparency and interpretability but struggle with capturing complex relationships [96]. Decision trees provide simplicity and ease of understanding but may have limited generalization and interpretability in tree ensembles [9]. K-Nearest Neighbors (KNN) models offer intuitive explanations based on similarity, but transparency depends on features and distance measures [61, 65]. Rule-based learning generates explicit rules for interpretation, but coverage and specificity can impact interpretability [101]. General additive models (GAM) provide interpretable representations, but modifications may affect interpretability. Bayesian models offer transparency through graphical representations, but complexity can hinder interpretability [96].

The interpretability of an AI model is closely tied to its complexity. In general, as the model becomes more complex, it becomes increasingly challenging to interpret and explain its behavior. One common obstacle faced in adopting this approach is the inherent trade-off between interpretability and accuracy. Balancing the need

for a clear understanding of the model's inner workings with its performance and accuracy poses a significant challenge [1].

**2.3.2 Post-hoc method.** In the realm of AI interpretability, an alternative strategy involves building a highly intricate and opaque black-box model that achieves exceptional accuracy. Afterward, a distinct set of techniques can be employed to provide explanations in a post hoc manner. Although this approach can be complex and resource-intensive, a substantial portion of recent advancements in explainable AI falls within the post hoc category [40]. These advancements encompass various forms of elucidation, such as explanations expressed in natural language [77], visual representations [88] of learned models, and other explanatory methods [95].

There are three renowned post-hoc methods in Explainable Artificial Intelligence (XAI): LIME, SHAP, and GradCAM. These techniques have gained popularity for their ability to provide interpretability in black-box models. LIME [119] focuses on generating explanations for individual predictions by approximating a black-box model locally using interpretable surrogate models. It excels in providing local interpretability but can be computationally expensive and lacks a global perspective. It can identify features that humans find difficult to understand, but its perturbation method can cause a small input variation to result in a large output change. This makes the network's explanations susceptible to manipulation through simple transformations [74]. SHAP [87], on the other hand, is a unified framework based on cooperative game theory that assigns feature importance values to explain model predictions. It offers both local and global interpretability, handles feature interactions well, and satisfies desirable properties such as fairness and consistency. However, it can be computationally demanding and may not scale well to large datasets. GradCAM [124] utilizes gradient information to highlight important regions in an input image, enabling visual explanations for deep learning models. It is particularly useful for computer vision tasks, providing intuitive and actionable insights. However, it is limited to visual explanations and may not capture complex relationships between features.

**2.3.3 Sensor data XAI.** While the main inputs for LIME and SHAP are the model's input and output [9], LIME and SHAP may struggle to capture complex feature relationships compared to GradCAM. LIME approximates the black box model with local surrogate models that may not fully capture intricate interactions. SHAP assigns feature importance values but may miss intricate feature interplay. In contrast, GradCAM's visual approach directly utilizes gradients to highlight important image regions, providing a more comprehensive understanding of feature relationships, especially in computer vision tasks [18, 63].

Considering that GradCAM is primarily designed for computer vision tasks [124], an interesting question arises regarding its direct applicability to sensor data. Certain research endeavors aim to modify sensor data into a semantic "image" matrix format in an attempt to adapt it to the mechanisms utilized by GradCAM [10]. This is due to the inherent difference in input data types between GradCAM, which operates on pixel-wise image data, and sensor data, which often consists of multiple channels generating different types of input data.

In this work, we aim to tackle this issue by developing an explanation method specifically tailored for sensor data. Our approach seeks to leverage the underlying mechanisms of GradCAM while accounting for the unique characteristics and complexities present in sensor data.

## 2.4 Synthetic Vision Domain Description

The creation of synthetic images is a critical technique for technologies such as virtual and augmented reality or other sensors that can generate a precise digital world for humans to interact with. While images may not be the most efficient means for smart space systems to comprehend the physical environment, they are certainly the most effective way for humans to grasp and interact with sensor data. Synthetic visual data possesses comparable characteristics to genuine data, enabling it to accurately depict a digital world.



Visual output from sensor data offers several advantages that make it a compelling choice over natural language output for certain applications. One of the key advantages of visual output is its ability to capture non-verbal context and subtle details that may be challenging to convey through text alone. Visual information provides a comprehensive representation of spatial relationships, postures, and interactions within an environment, enabling users to gain an immediate and holistic understanding of the situation [50]. Moreover, visual representations, such as images or videos, can transcend language barriers and be universally understood, regardless of linguistic background. This is especially valuable when dealing with multilingual audiences or when aiming for widespread dissemination of information [78].

In addition to being more intuitive and easily interpreted, visual output is less prone to the ambiguity inherent in natural language descriptions. It offers greater precision in conveying specific details and captures temporal information, allowing for the continuity of motion and changes over time to be better represented [51]. Visual output also facilitates enhanced data fusion by integrating information from multiple sensor sources into a coherent representation. Certain tasks, such as surveillance, anomaly detection, and behavior analysis, inherently rely on visual cues, and visual representations can directly support decision-making in these scenarios.

While visual and language outputs each offer unique advantages, they are not mutually exclusive; in fact, they can be highly complementary. By combining visual and language outputs, a sensing system can provide a rich, interpretive, and explanatory view of sensor data that leverages the strengths of both modalities. Visual output offers an intuitive and holistic view of spatial and temporal dynamics, while language output provides descriptive and contextual information in a human-readable form. Together, they create a more comprehensive and accessible representation of sensor data, facilitating enhanced communication and understanding for many users and applications. The fusion of vision and language thus offers a powerful approach for enhancing the explainability and interpretability of complex sensor data.

One of the most related booming areas is image generation via text. It generate synthesis image from text based image generation technique [23, 47, 67, 90, 116, 117]. The development of DALL-E2 [102] has revolutionized text-to-image models [110] by introducing a new level of creativity and sophistication. Unlike previous models, which often produced limited or generic images based on textual descriptions, DALL-E2 has the ability to generate unique and imaginative visuals that go beyond what is explicitly stated in the text. This breakthrough has opened up new avenues for creative expression and has the potential to transform industries such as design, advertising, and entertainment. Diffusion model which improves these previous results via diffusion method that beat the state of the art result [39]. Not only texts, sensors that have more real-life "descriptions", also need to derive explainable vision domain features for humans to interact with. The representation of sensor data as an image has been a subject of increasing attention and significant focus [58]. Various methods [45, 83, 131] have been attempted to convert sensor data into an "image," but none of them produce actual images. Instead, these methods are primarily based on natural language processing (NLP) and signal graph techniques.

Based on the state-of-the-art vision synthetic method. Our work contributes a heuristic sensor domain explainable deep generative method to the community.

### 3 METHODOLOGY

To provide an in-depth understanding of our research, we illustrate more details of background knowledge and design of our work in this part.

#### 3.1 Overall Structure

To begin, we constructed general purpose sensors [81] that are multipurpose and incorporate a majority of the non-invasive sensors available, with adjustments made by us to enhance sensor-wise explainability and safeguard privacy.

In this work, we first built general purpose sensors [81] that contains most of the noninvasive sensors on the board and makes our own modification for channel contribution analysis and privacy protection purpose. Subsequently, we placed the sensors in a room where regular activities occur. We utilized data gathered from users as both a training and testing set to confirm the effectiveness and durability of our methodology (see Figure 3). Due to significant differences among sensor datasets, implementing transfer learning on sensor data is considerably more challenging than on image datasets. Therefore, the encoder component of our model was specifically designed to facilitate small dataset learning without requiring transfer learning techniques. We trained the encoder of our model using the data we gathered. Once the 20 activities were accurately classified, a sensor activation map was produced to aid users in comprehending the data. Concurrently, a sensor data representation matrix was generated from the encoder and used to provide visual explanations in the decoder component of the model. This innovative approach, which offers comprehensive sensor analysis and visual explanations, has the potential to effectively analyze complex combinations of daily activities. This system can assist individuals without professional expertise to gain a multifaceted understanding of smart space sensor data.

In order to bolster the credibility of our approach, we also applied our method to a well-known publicly available dataset [118] related to sensors. The dataset we used for this comparison has a dissimilar sensor configuration and sample size as compared to our dataset. Furthermore, it is much larger in size when compared to our own dataset. Our experiments on the public dataset aimed to evaluate the impact of varying sensor dataset sizes on machine learning outcomes. Furthermore, we aimed to demonstrate the generalizability of our method to diverse data types generated by sensors with different configurations. The results of our experiments demonstrate that our method is a promising approach towards developing a comprehensive system for explaining sensor data.

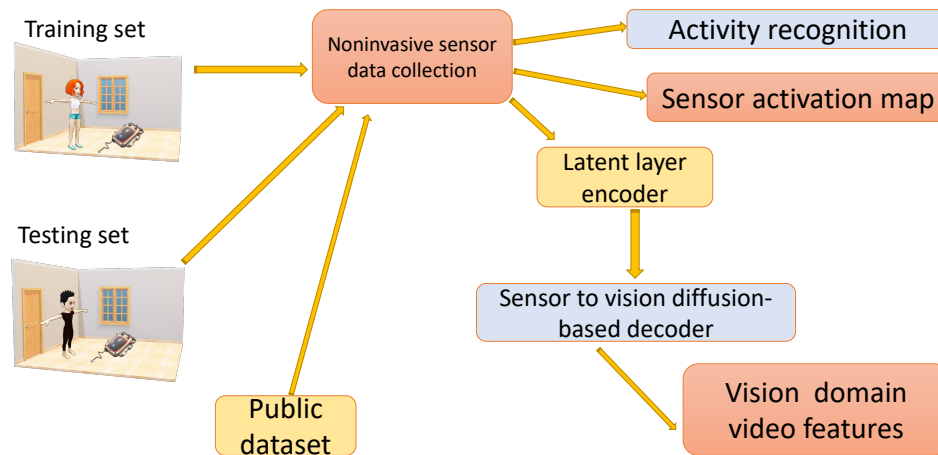


Fig. 3. The overall structure of our framework. The noninvasive sensor collects nonvisual data that describe events happening in the smart space. The model translates these non-intrusive data to vision domain explainable video features for users without the expertise to understand. Both our dataset and the public dataset are adopted for generalizability purposes.

## 3.2 Data Collection

**3.2.1 Challenge description .** As highlighted in the preceding section, general-purpose sensing is crucial. In order to enhance the generalizability of our approach, we developed our sensor based on insights drawn from prior

research [81]. However, upon this research, we found that the microphone was identified as one of the two most valuable sensors on the board due to its high sample rate and machine learning feature metrics. This led us to question whether the performance of the sensor is heavily dependent on the high frequency of the sound wave.

Another issue of concern pertains to the fact that the above sensor collects high-fidelity sound signals. As a result, it is possible for normal activities such as chatting or watching TV to be inadvertently leaked via this channel, thus raising new concerns about privacy breaches. This is particularly concerning in scenarios where sensitive conversations or private activities are taking place. The potential for this data to be intercepted and misused raises serious ethical and legal questions, particularly in light of the increasing use of smart home devices and the Internet of Things. Therefore, it is important to implement robust privacy protection measures.

*3.2.2 Sensor Design.* After analyzing the aforementioned discussion, it is apparent that our goal is to construct a device that enhances the generalizability of sensor data explanation while also safeguarding user privacy for their convenience. The collection of sensors comprises the majority of non-invasive channels capable of detecting human activities within the room. Our devices include PIR (motion), IMU (accelerometers), audio, GRB, pressure, humidity, magnetometer, and gas, and temperature sensors. These sensors are readily available and widely used, making them a prime candidate for generalizing smart space sensing capabilities. This device will be installed in the environment and does not involve any wearable sensors.

Most smart space sensors produce two types of output: binary output and continuous output in a range. Passive infrared (PIR) sensors, magnetic switches, piezo sensors, and passive RFID tags are some examples of binary sensors. These sensors typically have two possible states, which are "on" and "off." The transformation of raw data from environmental sensors into meaningful semantic states is a straightforward process, which is why some researchers prefer to use it directly for data representation [45]. While binary sensors can easily indicate the status of the environment, they may not be adequate for machine learning when it comes to analyzing more complex activities [10]. The only type of sensor on our device that functions as a binary sensor is the PIR sensor. When a PIR motion sensor detects any movement, it transmits an "ON" signal, and shortly after the motion stops, it sends an "OFF" signal. Accelerometers are a type of inertial sensor that provides continuous output, usually indicating movement along the X, Y, and Z axes. They are commonly worn on the body to track movement [3, 115, 144]. We utilize accelerometers as environmental sensors to detect vibrations in the surrounding area. For instance, pouring water creates a different vibration frequency compared to running. By measuring vibrations along the X, Y, and Z axes at a predefined location, we can analyze the vibration pattern and determine its direction simultaneously. The RGB channel is capable of detecting colors within a specific range. For instance, if a person wearing red clothing sits next to the sensor, only the red (R) channel will be activated. On the other hand, if a person wearing yellow clothing is present, both the green (G) and red (R) channels will be activated simultaneously. The pressure sensor is capable of measuring barometric pressure, which varies with altitude and can provide valuable information about weather patterns, as well as the behavior of gases and liquids. Barometric pressure also has an impact on human health and changes in it can be used to forecast weather conditions, as it is often linked to the movement of air masses and the creation of weather fronts. The readings from a pressure sensor can also provide insights into the indoor air quality, especially when activities like heating, ventilation, and air conditioning are in operation. By monitoring changes in air pressure, the sensor can detect whether the HVAC system is on or off and provide information about the circulation and quality of air within the indoor environment. The magnetometer is a sensor that detects the strength and direction of magnetic fields. However, its readings can be influenced not only by electronic devices in close proximity but also by human activity. This is because the human body contains a high proportion of water, which can absorb energy when exposed to radio frequency (RF) electromagnetic fields. Therefore, human activity close to the magnetometer can also cause magnetic interference and affect its accuracy [17, 91]. The gas sensor is capable of detecting Ethanol, Alcohol, and Carbon Monoxide in the air, making it useful for air quality measurements. If a person is running

heavily in the room, the gas sensor may identify an obvious change in the air quality levels compared to normal readings.

To ensure privacy, we have lowered the frequencies of all channels to approximately 98HZ. Additionally, the rate at which we detect activities is 90HZ. Furthermore, we aim to establish an equal contribution analysis by setting up the same sampling rate of 90 HZ for each channel, which is different from previous works. The previous sampling rates for the microphone and accelerometers were 16KHz and 4KHz, respectively. It is important to note that Shannon's sampling theorem states that information contained in frequencies greater than half the sampling rate cannot be retrieved [12, 73, 100]. As a result, the original sound can not be fully recovered.

Based on this device, we collect data for sensor-wise analysis. We describe the detail of our dataset in the chapter 4.1.

### 3.3 Sensor Encoder

**3.3.1 Problem statement.** In our sensor design, we have incorporated a greater number of sensors in order to create a more versatile and multipurpose sensing device. Merely providing a synthetic vision description from the decoder is insufficient for non-expert users to gain a comprehensive understanding of how this system operates. The decoder's output of a running video can indicate that the activity of running has occurred, but it may not be sufficient for non-expert users to fully understand how the system works. For instance, a room designer may require more information on how specific factors are affected by this activity. They may need to determine if the humidity level needs to be decreased when someone is running, or if the oxygen level needs to be increased during this activity.

XAI has emerged as a valuable tool for elucidating deep learning models. As previously discussed, GradCAM outperforms LIME and SHAP. However, it is important to note that this technique is tailored specifically to image data. Unlike images, sensor data does not have a uniform pixel-wise input. This is because different sensor channels may contain data with varying data types. As a matter of fact, there is a growing need to develop similar XAI tools tailored for sensor data.

The small dataset dilemma is another challenge that researchers encounter in smart space activity recognition [123].

In the context of HAR using smart space sensors, it is important to recognize that each space has a unique set of visitors with varying activity patterns. As a result, the same activity can be detected by different sensors, and this can lead to variations in the data collected. For instance, consider a library and a gymnasium. While both places may have people walking or running, the frequency and duration of these activities can differ greatly. Similarly, in a classroom, students may be sitting for an extended period, whereas in a cafeteria, people may be standing or moving around frequently. These variations in activity patterns make it essential to tailor the sensor-based HAR models to each specific environment. In addition, varying sensor configurations across different smart spaces can also influence the data collected and subsequently affect the performance of the HAR models.

**3.3.2 Encoder Architecture.** The figure 3 illustrates the general structure of the encoder, which was trained by the author using a 20-activity classification approach. The second-to-last layer of the encoder was then passed on to the subsequent decoder part.

**3.3.3 Skewness Correction.** Prior to feeding the data to the model, a normalization step is performed using a larger dataset of daily life data. This is done to address any skew present in the sample data, as normalization is a form of data augmentation. Specific events can sometimes influence the data, leading to overfitting of the model. For instance, a 1-degree difference in the environment for two days in two activities performed by the same user may be identified by the model as a feature, leading to overfitting. However, when the data is placed in a larger context, such temperature fluctuations may be recognized as just a minor influence. Skewed data distribution can

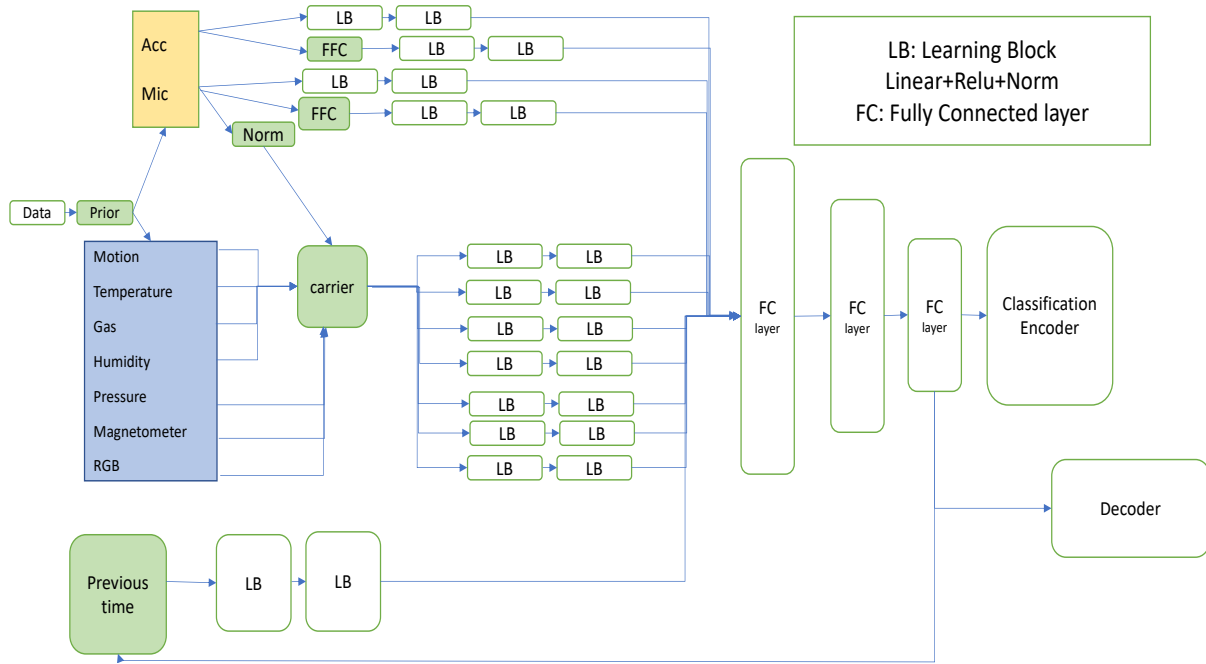


Fig. 4. The structure of our noninvasive sensor data encoder. It is pre-trained with classification tasks. And then extract the FC layer as the embedded input of the decoder. We will show the function of the green blocks in the experiments chapter, which shows our design proves a success on the encoder side.

impair the model’s decision-making ability in normal cases, limiting its ability to identify commonplace scenarios. In situations where the data distribution is skewed towards larger values, the model will be better equipped to recognize larger values than smaller ones.

There are mainly 2 types of data normalization we use here. one is data standardization. For the data that has a standard deviation close to 0 or smaller than 1, we use min-max normalization instead. The overall data normalization parameter is previously determined. The time of calibration is fixed. Its time complexity is neglectable compared to other parts of the model that needs to be trained. After the skew correction of the data set, the performance improves to a certain amount. The result is shown in the chapter 4

3.3.4 *Fast Fourier Convolution*. Fast Fourier convolution is a novel operator proposed by [30]. Later adobe [130] adopts this idea and proves a huge success in the computer vision community. However, nearly all of the later research on this novel structure is in the computer vision area. This paper tries to explore any possibilities that facilitate the development of a more explainable feature in the smart home sensor area. Incorporating the Fast Fourier Convolution into the model provides a differentiable component that enhances the interpretability of the overall system. Particularly for smart home sensor applications, a more robust operator such as the Fast Fourier Convolution is necessary for generating meaningful and generalizable features that can support human activity recognition. Human activities often exhibit distinct frequency and periodic characteristics, which motivated us to explore the potential of this operator for efficient and robust feature extraction in the domain of HAR. This includes filtering out irrelevant features from the input data.

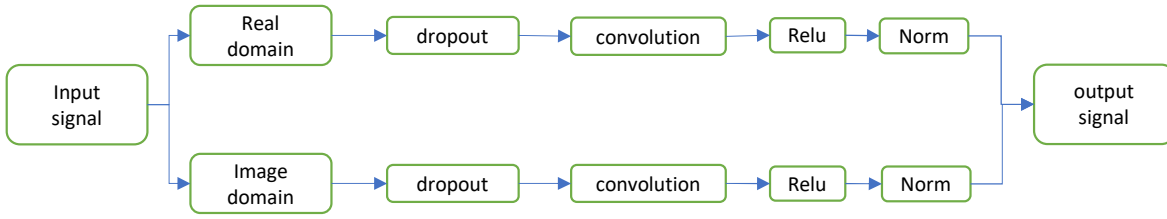


Fig. 5. The detail of Fourier dimension learning structure.

The provided pseudo code 1 outlines the steps involved in processing the input data using the Fast Fourier Convolution (FFC) technique. Initially, the real domain data is converted into the real and image domains through the Fast Fourier Transform. These two tensors are then combined for channel-wise detection. Since the input signal is a one-dimensional sensor signal, the detection stage is modified to employ one-dimensional convolution with normalization and the Rectified Linear Unit (ReLU) function, which enables the model to learn patterns in the Fourier domain data. Finally, the complex domain tensor is converted back into the real domain to facilitate processing in the subsequent layers. The figure 5 illustrates the model architecture of the FFC component. Further details on the performance of this approach can be found in the experiment section.

---

**Algorithm 1** Fast Fourier convolution on sensor data based on [30]

---

**Data:**  $x$  ;  
 $x_{image}, x_{real} = Real\_FFT(x)$  ;  
 $X = concatenate([x_{image}, x_{real}], dim = 1)$  ;  
 $x = Relu(BatchNorm(conv1d(x)))$  ;  
 $x = complex([x_{image}, x_{real}])$  ;  
 $x = irfft([x_{image}, x_{real}])$  ;

---

**3.3.5 Static Carrier.** There are 2 types of data fed into the model. Some of them like temperature, or pressure values are less fluctuating compared to the more dynamic channel like the audio channel. The statistical value is described in table 1. We calculate the Coefficient of variation value in the last column. The Coefficient of variation value is calculated in the equation 1. It describes how many deviations correspond to a unit of the mean value. A larger CV value means stronger fluctuations of the signal. If the channel's fluctuation tendency is too weak it will be hard for the model to identify any pattern from the raw data. The author designed this part with the concept of a "static carrier". The author selects the most fluctuated channel to "carry" the signal that is less dynamic. The less dynamic channel gets amplified and conveys more patterns than the author thinks. The equation 2 means an element-wise add from static tensor to tensor carrier. From our experiments, the add operator performs better than the multiplication operator. As a matter of fact, our work eventually uses add operator instead.

$$CV = \frac{\delta}{|\mu|} \quad (1)$$

$$new\_tensor = static\_tensor \oplus tensor\_carrier \quad (2)$$

Table 1. Channel-wise Coefficient of Variation (CV)

Channel	Mean	Std	CV
R	0.7808	0.9935	1.2723
G	0.6919	1.3002	1.8792
B	1.0502	1.8639	1.7748
AX	0.1026	0.9382	9.1371
AY	-0.0420	0.5836	13.8706
AZ	-0.0265	1.0613	40.0240
Gas	-1.5140	0.2002	0.1323
Humidity	0.0416	0.5884	14.14
Mic	-0.0249	1.2850	51.5822
MX	-1.2148	1.1244	0.9257
MY	0.0239	0.7011	29.372
MZ	0.1910	1.2572	6.5813
Pressure	-0.7433	0.1927	1.2278
Temperature	0.9133	0.4952	0.5422

The static tensor is selected from the largest value Coefficient of variation. The audio channel and accelerometer channel all have a CV value above 40. So we group these channels as dynamic channels. Other channels are grouped as static channels. The audio channel which has the largest value of CV can be used as a "carrier" that amplifies the changes in the static channel. As we can see in the figure 4, the blue part and yellow part represent the static and dynamic channels that will be processed separately. Our experiments show an improvement in the final performance compared to the model without this carrier.

3.3.6 *Previous Time Interval Recurrent Module*. Sequence transduction models are the basic model structure for time sequence analysis. A typical model like long short memory [54], gated recurrent model [31] or recurrent neural network [92] has long been applied to sequence transduction-related problems. Even for the state-of-the-art attention mechanism [136], the concept of "recurrent" still contains in its model design.

Based on previous experiences, this work also designs the encoder on a recurrent basis. The model detects the pattern based on the second-wise time interval. At the same time, it also feeds the previous 10 seconds hidden states together with the raw data into the encoder. The previous hidden state also slid second-wise. Suppose  $t(i)$  represents the data point corresponding to the second 'i', and let  $h(i)$  denote the hidden state of the i-th second. So the input  $x(i) = [t_i \rightarrow h_{i-1} \rightarrow \dots \rightarrow h_{i-10}]$ . So the target here is to map  $f(x(i))$  to an event space that can produce explainable features for the user.

The figure 6 shows the structure of the recurrent part. Each second-wise output will be part of the hidden state for the next stage input. This part provides a much more specific "context" for the model to understand the environment. The experiments show it contributes to the detection accuracy. This output hidden state is also the embedded input for the decoder.

3.3.7 *Small dataset issue*. We observed that CNN is a commonly used technique for handling smart space sensor data [10, 108], and there is a recent emergence of transformer-based models being employed for this purpose [114]. Research on small datasets is often given less attention. we opted for a simpler approach using MLPs due to the smaller size of our dataset. We believe this approach can provide efficient and satisfactory results for our task.

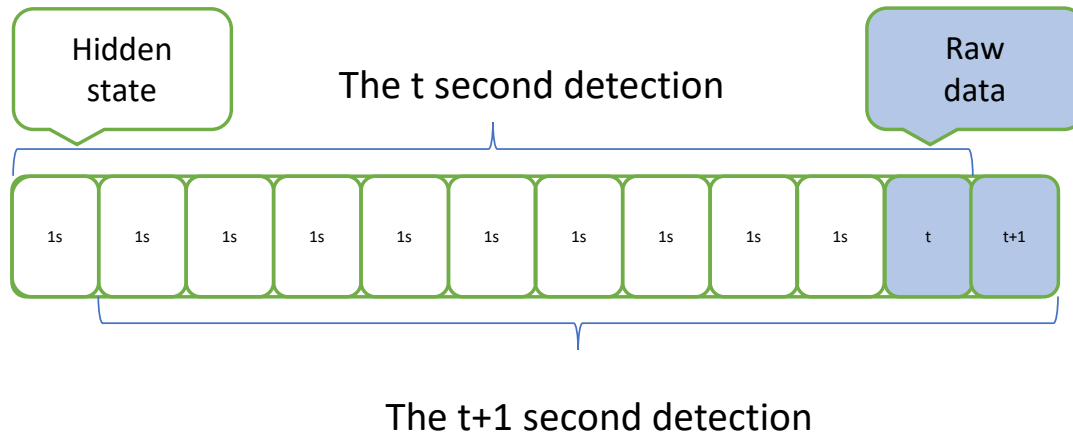


Fig. 6. We design our recurrent structure by sending the previous 10 seconds' latent states as part of the input for the next second's activity detection. We also use this hidden state as the embedded vector of the decoder part.

The Transformer has demonstrated impressive results on large-scale image datasets, outperforming traditional convolutional neural networks (CNNs) in several cases. However, when it comes to smaller datasets, Transformer's performance tends to lag behind that of similar-sized CNNs such as ResNet [125, 128]. Compared to the straightforward matrix multiplication used in MLPs, convolution involves additional steps such as cost reduction and specialized implementation, making it a more intricate process. It can be more computationally expensive and time-consuming [134]. In certain scenarios where the dataset is small, the performance of a single-layer MLP model has exceeded that of a multi-layer CNN model [69].

Given the small size of our sensor dataset and our aim to achieve an efficient solution, we decided to design the learning block using a simple MLP architecture. MLPs, due to their linear structure and basic mathematical operations, can be faster to train and easier to interpret compared to more complex architectures such as CNNs. However, to ensure that our choice of model design is effective and justified, we conducted an ablation study as part of our experiments. This involved removing certain components of our model one by one and analyzing the resulting performance to assess the contribution of each component to the overall accuracy. By doing so, we were able to verify that our decision to use an MLP architecture was appropriate for our dataset and that it could achieve satisfactory results without the need for more complex models.

### 3.4 Sensor Activation map

The preceding discussion indicates that GradCAM is a highly effective technique for explaining non-readable human activity data, including data captured by smart space sensors [64]. However, it is only applicable to CNN models that do not have fully-connected layers. This ensures that the model's complexity is not compromised, which may be necessary for achieving higher performance. The last convolutional layer in a CNN is where the most important features are found. GradCAM uses gradient information to determine the importance of each neuron for a specific decision, making it best suited for this layer [62, 124]. Since GradCAM was originally developed for explaining convolution-based image data, many related studies have attempted to either convert their sensor data into images or configure their models as convolution-based neural networks [7, 10, 62, 64, 71].

The issue described above suggests that a convolution-based solution may not be appropriate for our network due to both the small size of the dataset and the variability in inputs across different sensors. We design our model



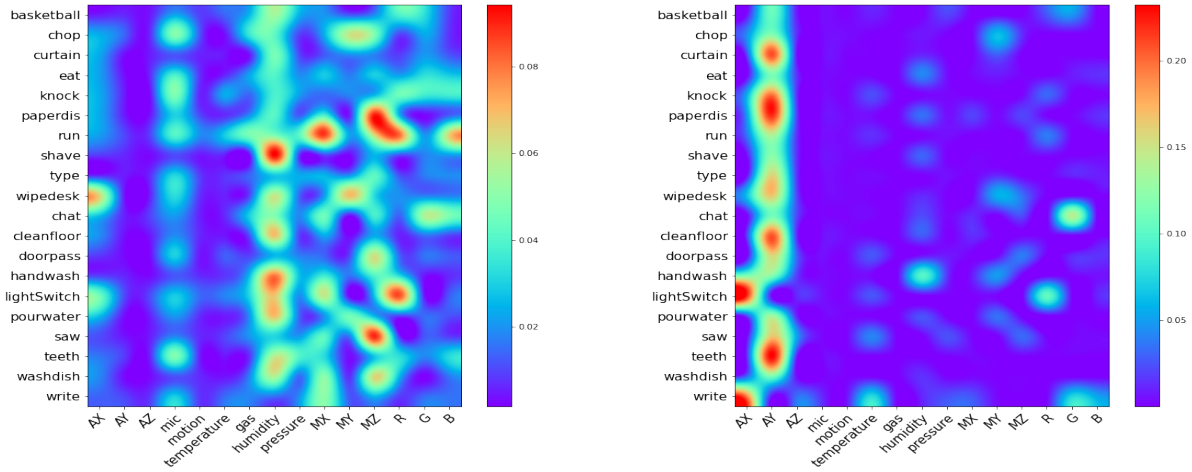


Fig. 7. Higher(left)/Lower(right) layer **gradient** based sensor-wise activation map

also grounded on the idea that the layer just before the fully connected one is the optimal option for capturing crucial features. So before this layer, a channel-wise design is helpful to trace back different types of sensor data even without convolution and uniform input channel. Since there is no dimensional transformation prior to the fully connected layer, we can utilize the weight and channel-wise gradient for each activation map without any intermediary steps.

We consider the problem of computing the neuron importance weights for our model. These weights correspond to the gradient of the feature map  $A_l^k$  with respect to the final class score  $y^c$ , where  $k$  represents the sensor channel and  $l$  represents a one-dimensional index over all elements in the feature map.  $Z$  is channel wise normalization factor. The neuron importance weights allow us to determine the contribution of each channel in the feature map to the activation of the current class 3.

$$\alpha_{A,k} = \frac{1}{Z} \sum_l \frac{\partial y^c}{\partial A_l^k} \quad (3)$$

To gain a deeper understanding of our model's design, we also investigate the lower layers of feature representation. Specifically, we compare the gradients of the input to the overall classification score with those of the higher-level layer features to the overall classification score. This analysis enables us to assess the relative importance of the lower versus higher-level features in the model's classification decision.

Based on the activation map 7, it appears that similar to the image model, the sensor-based model exhibits higher-level semantic features in the upper layers compared to the lower layers. The activation map provides a more plausible explanation of the higher-level features. For instance, the gas channel appears to contribute more prominently to intense running, while higher humidity levels are associated with hand washing and pouring water or activities that occur in the washroom, such as shaving. Additionally, the vibration patterns captured by the accelerometer and microphone are distinct for different activities, When each channel has an equal frequency rate.

Furthermore, we assessed these features using our decoder to gain additional insights into the impact of each individual feature in the experiments (Table 4).

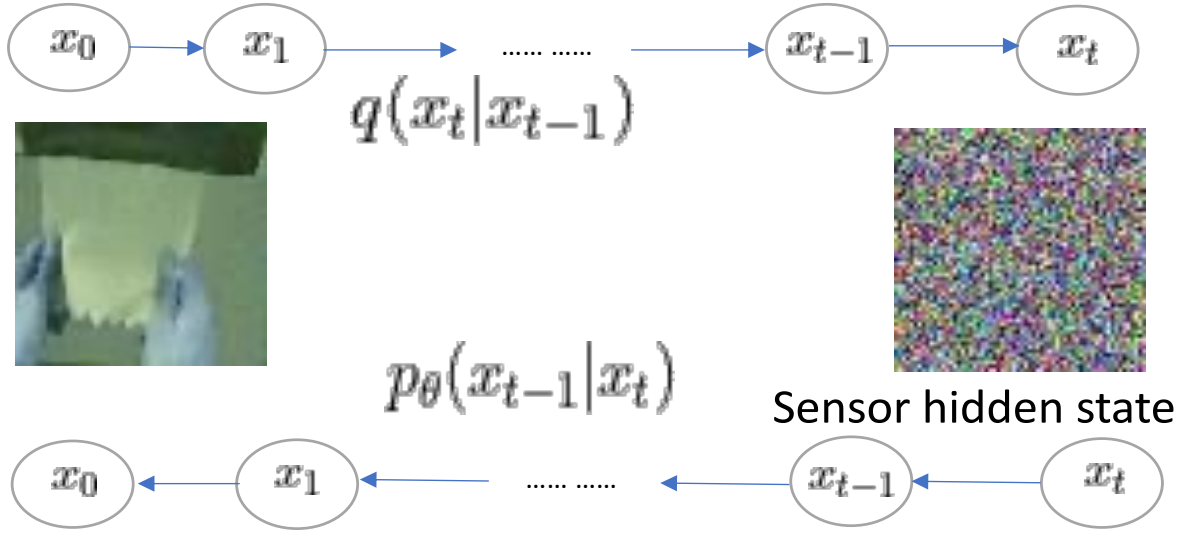


Fig. 8. The main structure of the sensor data decoder. The diffusion-based decoder extracts noninvasive sensors' data features and converts these features to the vision domain video features. The example here shows the sensor detects people pulling a paper from the paper dispenser.

### 3.5 Vision Domain Decoder

The encoder component of the model has effectively identified patterns in the activities, and the decoder is then used to extract interpretable features. The ultimate goal of this approach is to use it as a means of translating sensor data into the visual domain, in a novel and sophisticated manner. The main architecture of the decoder part is shown in the figure 8, which demonstrates one of the results that a vision domain paper dispenser activity translated from sensor data. Initially, we provide the unprocessed data to the encoder, and subsequently, we input the resultant embedded latent vector to the decoder. Finally, the decoder translates this latent vector into the visual domain.

**3.5.1 Conditional Diffusion Model.** In our method 8, Our problem can be described as a Markov chain where information diffuses forward T steps from the sensor space to the vision space 4. The  $q(x_{1:T}|x_0)$  in the equation is also defined as the trajectory of the forward process. The current step is only defined by the previous step. The figure 8 indicates the forward process in the first row. The  $q(x)$  means the real data distribution, in our case is the vision domain representation of each activity. Each step of this Markov chain gets a new latent vector by adding noise to it 5. The forward process gradually approximates the distribution we want. For the unconditional generative model, the forward process usually approximates a normal distribution. The new Gaussian distribution parameters mean is defined by the  $\mu_t$  and variant defined by  $\Sigma_t$ . The  $\beta$  can be a scheduler or a constant during the forward process. The  $\beta$  can be learned by reparameterization if it is not fixed.

$$q(x_{1:T}|x_0) = \prod_{t=1}^T q(x_t|x_{t-1}) \quad (4)$$

$$q(x_t|x_{t-1}) = N(x_t; \mu_t = \sqrt{1 - \beta_t}x_{t-1}, \Sigma_t = \beta_t I) \quad (5)$$

Next, we need the generative model to produce different activities based on different sensors' signals that describe the current smart space state. The conditional model can be formulated in the equation 6.  $y$  denotes the condition of the model. For example, if there is someone running in the smart space. The smart sensor may detect this activity and send it to the explainable system which is the diffusion-based decoder in our model. Instead of starting from noise, our encoder sends latent variables to the decoder 4. The learning equation 7 adds a term that indicates the gradient for the conditional function [39]. The reparametrization function for the conditional generative model is equation 8.

$$p_\theta(x_{0:T}|y) = p_\theta(x_T) \prod_{t=1}^T p_\theta(x_{t-1}|x_t, y) \quad (6)$$

$$\nabla_{x_t} \log p_\theta(x_t|y) = \nabla_{x_t} \log p_\theta(x_t) + s \cdot \nabla_{x_t} \log p_\theta(y|x_t) \quad (7)$$

$$\hat{\mu}(x_t|y) = \mu_\theta(x_t|y) + s \cdot \sum_{\theta} (x_t|y) \nabla_{x_t} \log f_\phi(y|x_t, t) \quad (8)$$

Our sensor encoder is intended to generate a latent vector capable of capturing human activity information, which may pertain to either a single activity or multiple activities. The latent layer and noise video are sent to the diffusion model. The SNR can be expressed in the form of  $\log SNR \lambda_t$ . We also use the adjusted denoise model [53] that applies a weighting function to the loss.

We begin our work by focusing on the classification of single activities, as it is the starting point of our research. Our dataset comprises 20 activities, while the public dataset contains 9 activities. To ensure the robustness and generalization of the encoder, we had two individuals perform each activity in our dataset for both training and testing purposes. The embedded sensor vector was used as a guide for the model to identify the relevant explanations in the visual domain. Furthermore, our experiments demonstrate the potential for generating multiple activities when the sensor is uncertain about what is occurring in the smart space. We will delve into this topic further in the upcoming section. In the public dataset, we have 9 subjects conducting 11 activities. We also translate these sensor data with a conditional diffusion model. Our results also indicate success in applying our approach to the public dataset.

Based on the model structure [53], we design our 3D Unet model with Fast Fourier Convolution (see Figure 9). The corpus available for training with this type of data is not as extensive as that of GPT-3. Various sensors exhibit distinct data properties, sampling rates, and channels. Decoding it directly is not stable; therefore, we filter our sensor data with the Fast Fourier Kernel using our structure. Compared to the traditional 3D Unet, we also have Faster Fourier convolution in the 3D Unet block. This optimizes the symmetric structure on both ends. The downsampling and upsampling procedures also incorporate a transformer component. The model studies the Fourier domain pattern with convolution kernel for both sides. It means the data stream of the sensor side and the visual side are all get optimized. The sensor encoder is responsible for transforming raw sensor data into a feature representation that can be effectively decoded by the decoder. Its design plays a crucial role in the overall performance of the system, as the encoder must capture relevant information while removing noise and irrelevant features. Therefore, a well-designed encoder can also improve the stability and accuracy of the

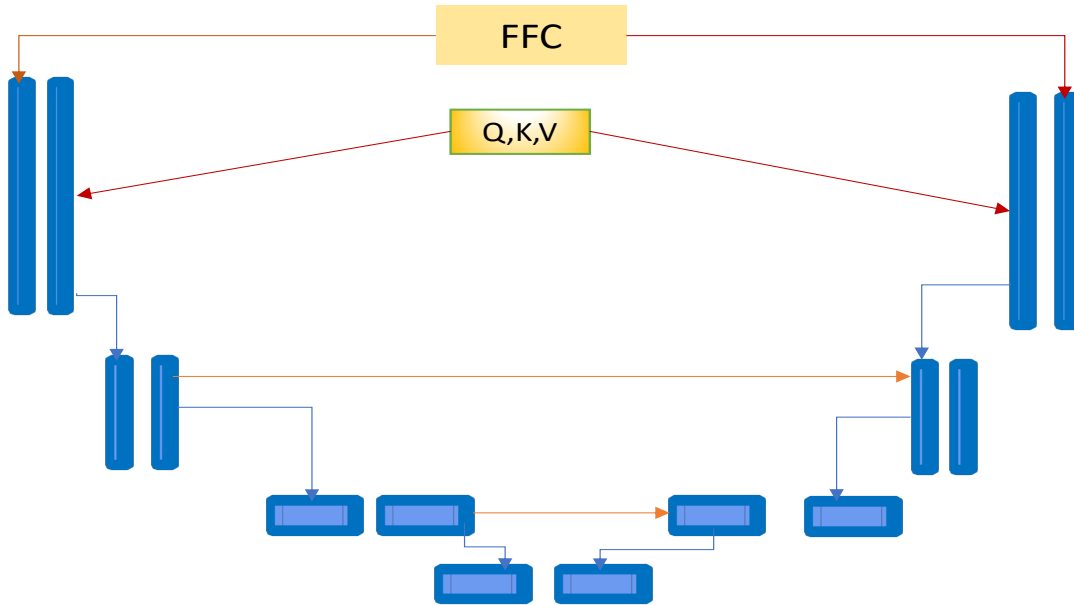


Fig. 9. Based on the 3D U-net structure [53], we design our FFC-based 3D U-net model that can successfully extract vision domain features from sensors' data and improve the result 4. Each block is a 4D tensor as  $frames \times height \times width \times channel$  the upsampling and downsampling blocks are adjusted by a factor of 2. We plug the FFC(Fast Fourier Convolution) module into the model to improve the diffusion side model.

system's output. The next chapter will present an ablation study for more in-depth analysis and understanding of this method.

## 4 EXPERIMENTS AND RESULTS

After the previous discussion of the related theory, we will provide the experimental evidence that supports our system. How we encode the sensor data and translate it to the vision domain. In this part, we also discuss the technical details of how we apply our model to a real-life sensor. Our method proves that our model can successfully translate the smart space sensor data into an explainable vision domain feature. Experiments' results show that it is possible to build a noninvasive general-purpose sensing system in the smart space and extract explainable features based on the events happening in the smart space.

### 4.1 Data Collection

As the main purpose of the work is vision domain feature extraction, we lower the number of subjects and increase the number of activities Table 2. We use a general-purpose sensor in a controlled smart environment to gather data on human activities. In the smart space, each resident carries out 20 distinct activities individually. The sensor collects data for training and testing sets. The 20 activities are playing basketball, chopping, moving curtains, door passing, eating, washing hands, knocking, switching the light, and paper dispenser, pouring the water, running, sawing, shaving, typing, washing dishes, wiping the desk, writing the board, brushing the teeth and chatting. Each activity comprises a 3-minute recording. 2 subjects participated in the data collection. To address the small dataset issue, we collect our dataset which is relatively smaller compared to the public dataset

Dataset	Sensor(s)	Number of subjects	Activities	Setup
PAMAP2	Accelerometer, magnetometer, gyroscope, temperature, heartbeat	9	11	Wearable
CASAS	Motion, temperature, magnetometer	20	9	Ambient
Our dataset	Motion, accelerometer, magnetometer, gyroscope, temperature, humidity, RGB, gas, pressure, MIC	2	20	Ambient

Table 2. Dataset comparison. The reason for the setup and dataset selection is discussed in part 4.1. We increase the number of activities in our dataset to focus on the vision domain feature extractions. we also use a public dataset to prove the generalizability of our method.

we use in the comparison group. Our work finally translates these non-invasive sensor data to vision domain features that can explain the activity for non-expert users.

#### 4.2 Public Dataset

To bolster the credibility of our experiments, we also utilize a renowned dataset of human activity, gathered through sensors in a smart space. In table 2 there are 2 public data sets that are based on smart space activity recognition. CASAS [35] is the most similar dataset to ours. However, there is no standard configuration for general-purpose sensing. To prove the generalizability of our model to the most, we decide to use PAMAP2. It has different sensors and data-collecting methods. It contains a larger number of activities. We decide to use PAMAP2 as our comparison group for the purpose of generalizability on different sensor types and different activities. PAMAP2 [118] is the well-known smart home activity recognition base line [2, 5, 11, 44, 70, 72, 86, 94, 109, 121, 141]. The data set is a sensor-based data set that collect human activity data for smart space activity recognition. Each subject wears 3 IMUs on their chest, ankle, and hand and a heart rate monitor. Each IMU contains sensors like a gyroscope, accelerometer, magnetometer, and temperature. This data set has 9 subjects that perform daily activities with the sensors in their daily life. There are 2 types of activities. One is the desired activities that are required from the experiments instruction, Another is the activities they conduct in the rest of their daily life. As the second part of the activities does not happen in all participants' life, it is not comparable. So we remove these types of activities like watching TV, doing computer work, folding laundry, house cleaning, and playing soccer. The main activities which are designed for each subject are fed to the encoder. This encoder is different from the previously mentioned encoder 4 because sensor channels are totally different from our device. The main activities are, lying, sitting, standing, walking, running, cycling, Nordic walking, ascending stairs, descending stairs, vacuum cleaning, ironing, and rope jumping. Our experiments show that our method can extract explainable features from other types of sensors. It gathered data for each of the 18 activities from 9 subjects, spanning a duration of 10 hours. Out of the 10-hour recording, 8 hours were labeled as 1 of the 18 activities performed during data collection. In addition to the variations in sensor setup, this dataset also provides diverse data sizes to enable a thorough investigation of the sensor aspect.

### 4.3 Encoder Result

**4.3.1 Our Data Set.** From the encoder structure (see Figure 4) above, we discuss the green block that helps to improve the final result. The figure 10 shows the result when we remove different parts of the design. The F1 score describes the data more precisely than the accuracy. So we use the F1 score, precision rate, and recall rate for comparison. The highest F1 score is our baseline. Its F1 score is 0.85 compared to the other group. All of the other F1 scores are under 0.8. The "NoFFC" group means when removing the Fast Fourier Convolution part, the F1 score is around 0.75. This proves FFC also improves the performance of sensor data. "nanocarrier" group means when removing the static carrier the F1 score is 0.78. We observed a decrease in performance when we replaced the method of amplification from addition to multiplication. As it is shown in the above table 1, we classify any coefficient of variation above 40 as a dynamic channel. If the Coefficient of variation is under 40 we group it as a static channel. We then add the static channel and dynamic channel together. We choose the mic channel as a static channel carrier, which has the highest Coefficient of variation. From the experiment result, We think the main reason this "carrier" works is that the high-frequency channel amplified the subtle change of the static channel. However, when changing the add operator to multiplication, the performance drop. From the "MulCarrier" group result, the F1 score drops drastically under 0.2. This means adding works better than multiplication. The "NoPrev" group removes the previous 10 seconds' recurrent block. Its performance also collapsed. The days of the ambient data collection as a prior component also help to boost the performance from under 0.2 to above 0.8. The training epoch is 120. The optimizer is Adam. There are two parameters of Adam which are coefficients computed running averages of gradient and its square. These 2 coefficients are normally set up as 0.9 and 0.999. However, from our experiments, the best performance is when these 2 parameters' values are 0.5 and 0.66. The standard result from the "Adam90" group in the bar chart is much worse compared to the baseline. To test the robustness of our model against the raw data from our device, we blend noise with different percentages to compare the possible influence (see Figure 12). When adding a different proportion of white noise to the raw data, the performance remains stable. This means the model is robust against various levels of noise. Each group's median F1 score is above 0.7. Most of the group fluctuates around 0.8. The percentage of noise influences the data more after 0.7 percent. These groups' performance fluctuates around 0.75. Except for different percentages of noise, we also reduce the frequency to see the influence on the model performance. From the figure (see Figure 13), we can see that the model performance decreases as the frequency rate decreases. After 20HZ, the F1 median score dropped from 0.7 to 0.57.

We conducted an ablation study of various models by replacing our learning blocks with different operators to evaluate their performance. Based on the discussion we had earlier, it is evident that for larger datasets, transformer or CNN models may deliver better results. However, our study shows(see Figure 11) that these models may not be suitable for a relatively small dataset like ours. Our final results corroborate this observation, where we found that these models did not perform well on our small dataset.

From table 2 we can see all the performance of 20 activities collect by our device, most of the activities' F1 scores are 1. However, there are 3 activities that can not be clearly identified. The chat activity performs worst. Its F1 score is 0.32. The precision and recall rate is also low. They are under 0.35. Pulling paper from dispenser activity also gets an F1 score which is under 0.5, the recall rate is lower. It means the number of false negative rates is higher. This also happens in pouring water activity. Its F1 score is also lower than 0.5. However, the false negative rate is much lower compared to the pouring water activity. This shows the encoder can detect most of the activities and can help the decoder to extract appropriate vision domain features for the next stage.

**4.3.2 Public Data Set.** We also apply our framework to a public data set to further demonstrate the generalizability of our framework. As it is mentioned above, we use PAMAP2, a famous smart space activity recognition sensor data set. Currently, there is no standard configuration for general-purpose sensing. The most important target is to prove that the diffusion method can extract explainable features from different sensors or data collection

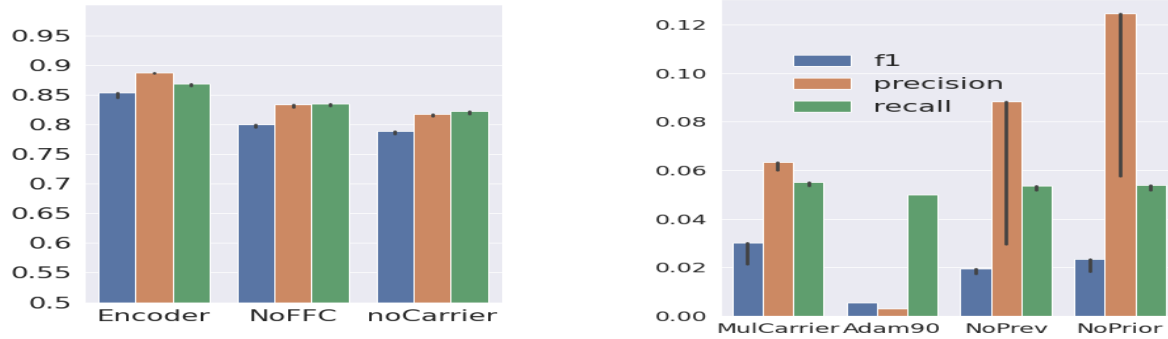


Fig. 10. Comparison of different structures. By removing the different green blocks we designed in figure 4, we can see our structure in the first group has the highest F1 score of 0.86 in the blue bar.

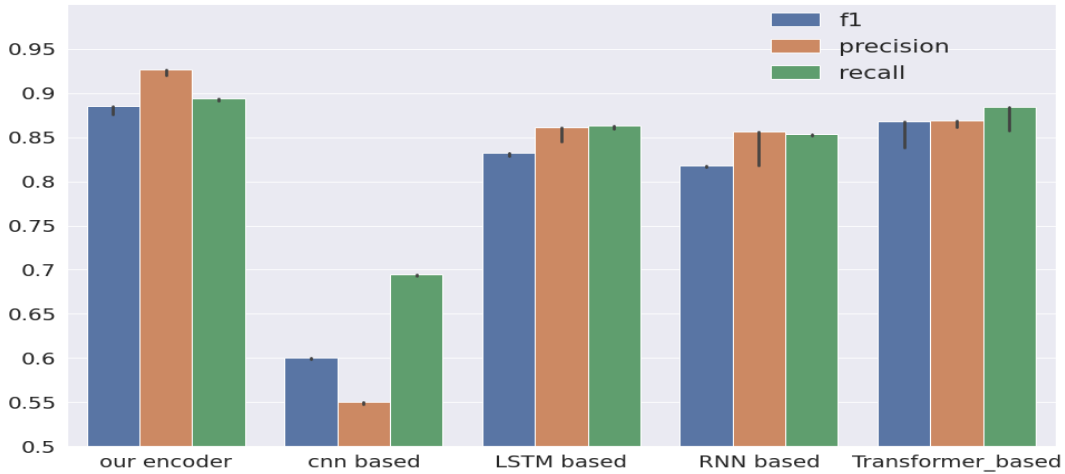


Fig. 11. Comparison of the encoder results reveals that our model performs better on smaller datasets.

methods. As a matter of fact, this part of the experiments is designed to prove the possibility of the diffusion method extracting explainable vision domain features from different non-invasive sensor data from different data collecting methods. Overlaps exist between our sensors and theirs. However, there are still different types of sensors. Another reason we select this data set is that it is different from our configuration and we still can apply the diffusion method to the raw data. Activities like running, and vacuum cleaning, can be successfully translated to the same vision features even if their sensors and way of collecting data are different.

The similar smart space ambient data set is CASAS [35], and the CNN-based model’s highest F1 score is 0.68 [10]. However, the highest CNN-based model’s F1 score of PAMAP2 is above 0.9 [122]. It is easy to know that the non-intrusive wearable sensor like in PAMAP2 has a better activity recognition rate than non-touchable non-intrusive sensors like in CASAS. But the main purpose of public data set introduction is to prove the

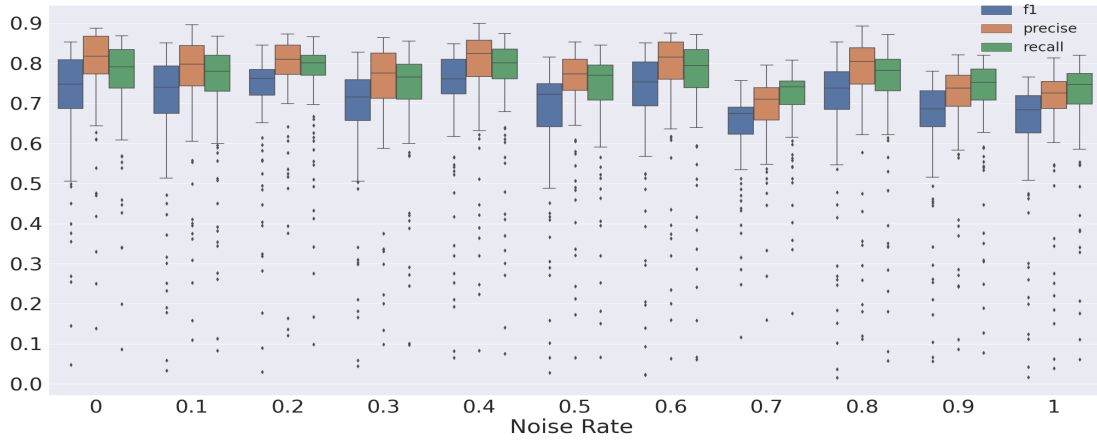


Fig. 12. Robustness against noise. The first group with an x-axis value of 0 means 0 percent of noise. This performs slightly better than other groups. The outlier samples also have a similar pattern between each group. This shows the robustness of our model against noise.

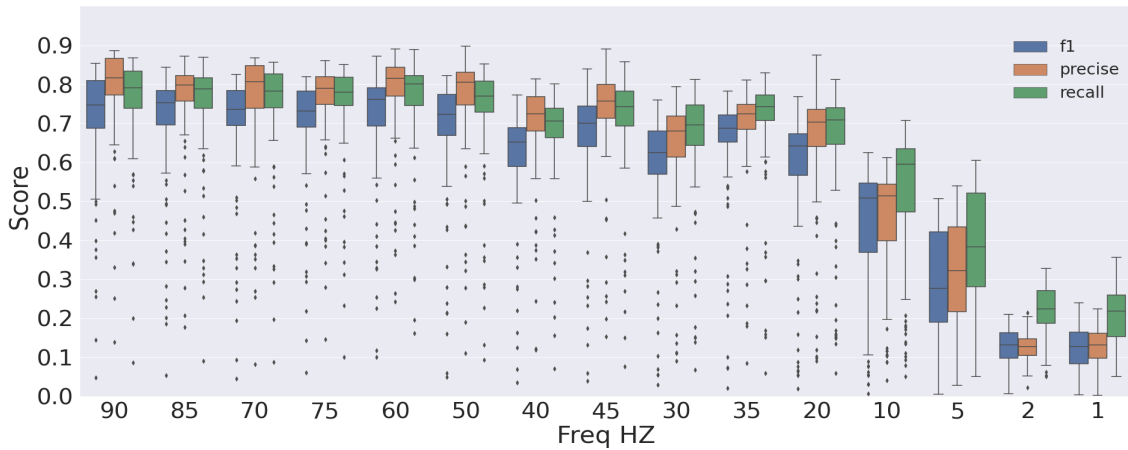


Fig. 13. Frequency influence of each group. We can see it decrease as the frequency drop down. The highest frequency rate is 90Hz. The lowest is 1 Hz.

generalizability of different sensors' setups. The CASAS sensors' setup is too close to our setup. we finally use PAMAP2 as a comparison group. More details about the data set are mentioned in the above section 4.1. The model structure here is a VGG alike model. With 3 stacks of convolution, pooling, and drop layers, we extract the



Activity Name	F1	Precision	Recall
eat	1.00	1.00	1.00
paperdis	0.43	0.50	0.38
write	1.00	1.00	1.00
chop	1.00	1.00	1.00
hand wash	1.00	1.00	1.00
pour water	0.48	0.50	0.47
clean floor	1.00	1.00	1.00
knock	1.00	1.00	1.00
run	1.00	1.00	1.00
curtain	1.00	1.00	1.00
light Switch	1.00	1.00	1.00
type	1.00	1.00	1.00
door pass	1.00	1.00	1.00
wipe desk	1.00	1.00	1.00
chat	0.32	0.33	0.31
basketball	1.00	1.00	1.00
saw	1.00	1.00	1.00
shave	1.00	1.00	1.00
wash dish	1.00	1.00	1.00
teeth	1.00	1.00	1.00

Table 3. Activity analysis. Highest detection rate for each activity, not in the same epoch. The overall highest F1 score within one epoch is 0.85

final dense layer as an encoder-embedded vector. And finally, we send the output of the encoder to the decoder model.

Additionally, we performed an ablation study [14](#) on different model architectures, this time using a much larger dataset size than the one we had collected. However, the comparable dataset size for our study was still small, such as CIFAR-10, making it challenging for the transformer-based model to perform well. In contrast, CNN-based models outperformed our model structure and transformer-based models. Interestingly, recurrent models demonstrated the best performance in this study.

#### 4.4 Conditional Diffusion Decoder Result

From the above encoder, the model then sends the embedded vector to the decoder side. We first describe each event with a 4-frame video. And translate the public dataset and our dataset with this vision domain descriptors. Our experiments show that we can successfully extract vision domain features from both of the datasets. Our initial result is based on the single events. For mixed events, it is still possible to extract vision domain features. we will also mention this part in the discussion section.

Frechet Inception Distance (FID) is a popular evaluation metric for generative models in the visual domain, and it is also a crucial measure for assessing video quality [\[8, 32, 52, 53, 76, 142\]](#). FID calculates the distance between the generated distribution and the real distribution in feature space, which is learned by the Inception V3 network trained on ImageNet. The lower the FID score, the better the quality of the generated result, as it indicates that

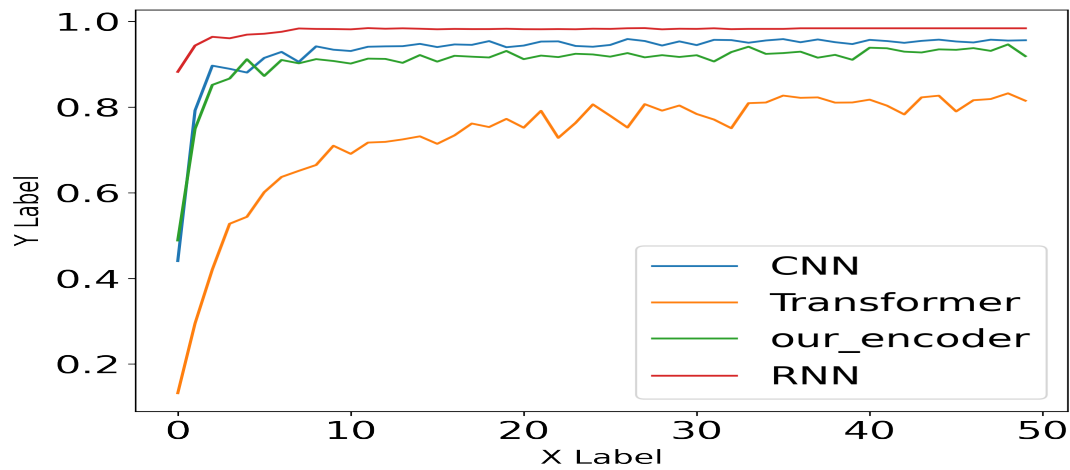


Fig. 14. Convolution works better on larger datasets. However, for PAMAP2 with a similar size to CIFAR10, transformers are still underperforming compared to other models.



Fig. 15. Vision Domain Video features extracted from our noninvasive sensor dataset. These activities are playing basketball, chopping, vacuum cleaning, curtain moving, door passing, eating, washing hands, knocking on the door, turning the switch on, paper pulling, water pouring, running, sawing, shaving, typing, washing dishes, wiping the desk, writing, teeth brushing, chatting. The people's face in the last chatting activity is blurred for privacy concern.

the generated distribution is more similar to the real distribution. FID is a popular metric in the field of Deep generative models and has been shown to correlate well with human perception of vision domain features [21].

Our sensor collects 20 activities and split them to train and test sets. The decoder translates these embedded vectors to different features (see Figure 15). Different sensors' data are all embedded in the same format in order to feed into the decoder side. For this sensor data-based diffusion model, we also design the 3D Unet block with a Fast Fourier Convolution kernel. This kernel also helps us to get a stable result. Confined by the computational resources, our first version of the video feature has a frame rate of 4 and a resolution rate of  $64 * 64$ . From the

result of our model, we can see that 4 fps can successfully show the variance of each frame. We also apply the training strategy [53] to use a lower resolution as guidance to the final output. We use a 32\*32 resolution rate video and extend the result to the 64\*64 final output for faster convergence.

Method	Resolution	FID-avg ↓
lower layer activation map	$4 \times 64 \times 64$	$13.45 \pm 0.1$
higher layer activation map	$4 \times 64 \times 64$	$11.72 \pm 0.2$
Without FFC	$4 \times 64 \times 64$	$8.43 \pm 0.2$
Ours	$4 \times 64 \times 64$	$7.9 \pm 0.1$

Table 4. Vision domain result based on different methods. Based on the results, it can be concluded that the performance of the decoder is enhanced by FFC. Additionally, the higher layers of the activation map exhibit superior performance compared to the lower layers. The baseline model is tested on the public dataset and our dataset

**4.4.1 Result of Our Dataset.** From the result (see Figure 15), it is evident that the decoder effectively utilizes visual domain features to accurately classify and describe the sensor data. As mentioned above in chapter 3.5.1, 3d Unet has an unstable issue. The experimental results (see Table 4) clearly indicate that FFC has improved the FID score of our model on both our dataset and the public dataset. There is also an ablation study of the performance of sensor-based activation maps in the decoder. With the metric correlating well with human perception of vision domain features [21], the evaluation corroborates the result in the chapter (see Figure 3.4) that a higher layer gradient map truly contains more explainable features compared to lower layer activation map.

**4.4.2 Result of Public Dataset.** To prove the generalizability of our data set, we also extract explainable features from the public dataset. This dataset's activities overlap with our dataset. There are 12 activities in the public dataset. We have vacuum cleaning, running in the public dataset and our dataset. New activities in the public dataset are ascending stairs, descending stairs, lying down, standing, walking, cycling, Nordic walking, ironing, jumping rope, and sitting. The purpose is to prove the model can translate the same activity with different sensors. The overall results are shown in the figure 16. Smart space areas may collect different datasets using various sensors, which can result in significant variations in model performance based on sensor type and dataset size. As discussed earlier, CNNs tend to perform better on this public dataset, while their performance on smaller datasets, such as ours, is suboptimal. However, based on our experiments, it is evident that the decoder performs well for different sensor encoders. This finding holds promise for developing effective sensor explainability methods in smart space applications.

## 5 DISCUSSION

In this part, discuss some limitations and concerns of our work.

### 5.1 Output Errors

During our training, we observe that there are also errors when the decoder generates the output video. From Figure 17, we can see more than one activity in one frame. We have "chatting" and "running" activities in one frame and "teeth brushing" and "typing" in another frame. This mistake happens when the model is not that sure what happens in the environment. However, this also provides a possibility that when there are multiple activities happening in one place, the model can still detect the new scene based on the limited training information we feed.

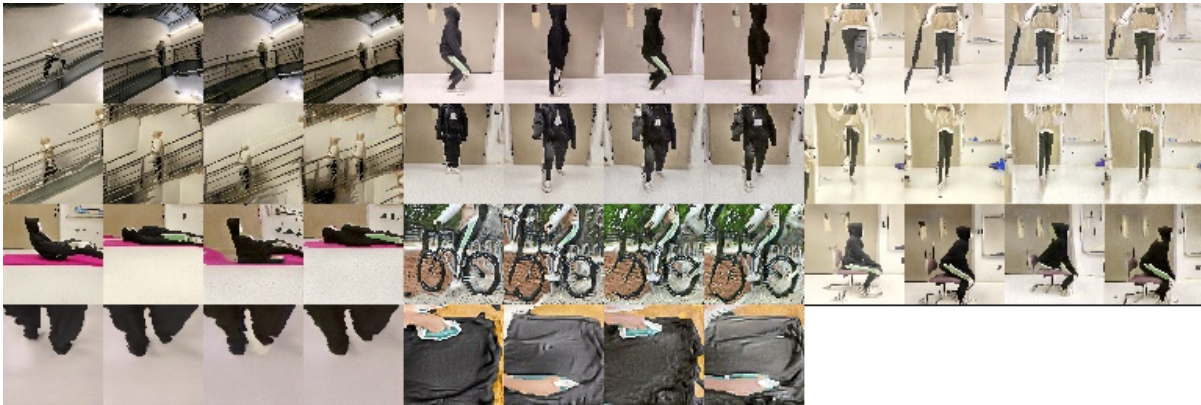


Fig. 16. Vision domain public dataset final video decoder results. They are stair ascending, stair descending, lying down, running, standing, walking, cycling, ironing, Nordic walking, rope jumping, and sitting.

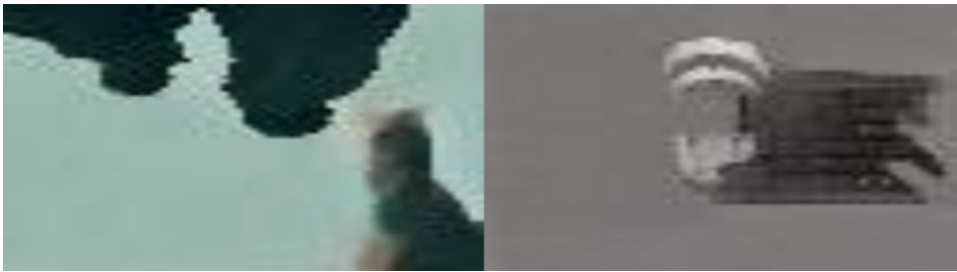


Fig. 17. One type of training mistake when the model is uncertain about which activity is happening, it gives us multiple activities' outputs. The left side shows both chatting and running activities. The right side shows typing and teeth brushing at the same time. This shows the possibility for multi activities feature extraction in our future work.

## 5.2 Multi Activity Scene and Model Imaginative Model

Our sensor data was collected for a single activity that occurs each time, but in real life, multiple activities may happen simultaneously, which can be a challenge for the model. However, our results, as shown in the figure 17, demonstrate that the model can generate scenes with multiple activities that were not present in the training set. Although this study focused on the initial vision domain explanation, we acknowledge the importance of considering multiple simultaneous activities in future work.

## 5.3 Different Sensors In Real Life

This paper exclusively employed a public dataset to test the generalizability of our work. Although the sensors used in the dataset were different from the ones on our device, there exist various types of sensors that we have not tested yet. Given that we have presented initial results in this paper, our future work will involve testing additional types of sensors in real-life settings to demonstrate their robustness against real-world events.

## 5.4 Privacy And Security

Another concern is that the sensor might be able to reveal the owner's activities in the smart space. As it is discussed in the previous paragraph, there is a possibility to generalize the explainable vision feature to all sensors. Our uniformly designed vision domain representation implies that all activities can produce the same output representation. For instance, when it comes to typing activity, the video representation can remain the same output, irrespective of the contents that the user types. As a result, our system can provide the user with a vision domain explanation while ensuring their privacy is protected.

## 5.5 Frames Per Seconds

As previously mentioned, our initial results effectively demonstrate the potential of vision domain features. However, in real-life scenarios where multiple activities occur within a smart space, we require a higher frame rate to capture subtle changes occurring at small time intervals. Due to constraints in computational resources, the initial results presented in Figure 15 were obtained using a frame rate of 4. At present, the variance between frames is adequately displayed. However, as we collect more activities in future experiments, increasing the frame rate could be a viable solution for our future work.

## 6 CONCLUSION

In this work, we present a framework that can extract explainable vision domain video features from non-invasive smart space sensors. Our work is based on the state-of-the-art deep generative model. To demonstrate the generalizability of our model, we conducted comprehensive experiments on both public and custom datasets. Our experiments show that our model structure can successfully improve the result. We also design a gradient sensor activation map for a small dataset like ours. We can also show explainable features on the sensor side. To provide a comprehensive explanation of smart space sensor data, we integrate features from both the sensor and the vision domain. Despite using different types of sensors, our framework can extract explainable features with consistent activity and accurately classify various activities. This is a promising initial result that can be generalized to more types of sensor data. Our model can provide explainable features to users. Our result also shows the possibility of multiple activities feature extraction. It shows the plausibility to explore an imaginative model for our next stage of work. More sensors will be deployed in the next stage of research.

## REFERENCES

- [1] Amina Adadi and Mohammed Berrada. 2020. Explainable AI for healthcare: from black box to interpretable models. In *Embedded Systems and Artificial Intelligence: Proceedings of ESAI 2019, Fez, Morocco*. Springer, 327–337.
- [2] Awais Ahmad, Anand Paul, M Mazhar Rathore, and Hangbae Chang. 2016. Smart cyber society: Integration of capillary devices with high usability based on Cyber-Physical System. *Future Generation Computer Systems* 56 (2016), 493–503.
- [3] Hamad Ahmed and Muhammad Tahir. 2017. Improving the accuracy of human body orientation estimation with wearable IMU sensors. *IEEE Transactions on instrumentation and measurement* 66, 3 (2017), 535–542.
- [4] Mohammad Abu Alsheikh, Ahmed Selim, Dusit Niyato, Linda Doyle, Shaowei Lin, and Hwee-Pink Tan. 2015. Deep activity recognition models with triaxial accelerometers. *arXiv preprint arXiv:1511.04664* (2015).
- [5] Belal Alsinglawi, Quang Vinh Nguyen, Upul Gunawardana, Anthony Maeder, and Simeon J Simoff. 2017. RFID systems in healthcare settings and activity of daily living in smart homes: a review. *E-Health Telecommunication Systems and Networks* (2017), 1–17.
- [6] Leila Amgoud and Henri Prade. 2009. Using arguments for making and explaining decisions. *Artificial Intelligence* 173, 3-4 (2009), 413–436.
- [7] Gustavo Aquino, Marly Guimarães Fernandes Costa, et al. 2023. Explaining and Visualizing Embeddings of One-Dimensional Convolutional Models in Human Activity Recognition Tasks. *Sensors* 23, 9 (2023), 4409.
- [8] Rajat Arora and Yong Jae Lee. 2021. Singan-gif: Learning a generative video model from a single gif. In *Proceedings of the IEEE/CVF Winter Conference on Applications of Computer Vision*. 1310–1319.
- [9] Alejandro Barredo Arrieta, Natalia Díaz-Rodríguez, Javier Del Ser, Adrien Bennetot, Siham Tabik, Alberto Barbado, Salvador García, Sergio Gil-López, Daniel Molina, Richard Benjamins, et al. 2020. Explainable Artificial Intelligence (XAI): Concepts, taxonomies,

- opportunities and challenges toward responsible AI. *Information fusion* 58 (2020), 82–115.
- [10] Luca Arrotta, Gabriele Civitarese, and Claudio Bettini. 2022. DeXAR: Deep Explainable Sensor-Based Activity Recognition in Smart-Home Environments. *Proceedings of the ACM on Interactive, Mobile, Wearable and Ubiquitous Technologies* 6, 1 (2022), 1–30.
  - [11] Ahmed Ayman, Omneya Attalah, and Heba Shaban. 2019. An efficient human activity recognition framework based on wearable imu wrist sensors. In *2019 IEEE International Conference on Imaging Systems and Techniques (IST)*. IEEE, 1–5.
  - [12] Oresti Banos, Juan-Manuel Galvez, Miguel Damas, Hector Pomares, and Ignacio Rojas. 2014. Window size impact in human activity recognition. *Sensors* 14, 4 (2014), 6474–6499.
  - [13] Ling Bao and Stephen S Intille. 2004. Activity recognition from user-annotated acceleration data. In *Pervasive Computing: Second International Conference, PERVASIVE 2004, Linz/Vienna, Austria, April 21-23, 2004. Proceedings 2*. Springer, 1–17.
  - [14] Akram Bayat, Marc Pomplun, and Duc A Tran. 2014. A study on human activity recognition using accelerometer data from smartphones. *Procedia Computer Science* 34 (2014), 450–457.
  - [15] Chris Beckmann, Sunny Consolvo, and Anthony LaMarca. 2004. Some assembly required: Supporting end-user sensor installation in domestic ubiquitous computing environments. In *International Conference on Ubiquitous Computing*. Springer, 107–124.
  - [16] Maik Benndorf, Frederic Ringsleben, Thomas Haenselmann, and Bharat Yadav. 2017. Automated annotation of sensor data for activity recognition using deep learning. *INFORMATIK 2017* (2017).
  - [17] Paolo Bernardi, Marta Cavagnaro, Stefano Pisa, and Emanuele Piuzzi. 2000. Specific absorption rate and temperature increases in the head of a cellular-phone user. *IEEE transactions on microwave theory and techniques* 48, 7 (2000), 1118–1126.
  - [18] Aditya Bhattacharya. 2022. *Applied Machine Learning Explainability Techniques: Make ML models explainable and trustworthy for practical applications using LIME, SHAP, and more*. Packt Publishing Ltd.
  - [19] Ulf Blanke and Bernt Schiele. 2009. Daily routine recognition through activity spotting. In *Location and Context Awareness: 4th International Symposium, LoCA 2009 Tokyo, Japan, May 7-8, 2009 Proceedings 4*. Springer, 192–206.
  - [20] bloomberg. 2023. Samsung Shares Vision to Bring Calm to the Connected Device Experience at CES 2023. <https://www.bloomberg.com/news/articles/2023-01-04/samsung-launches-smart-home-hub-pushing-deeper-into-amazon-turf>
  - [21] Ali Borji. 2022. Pros and cons of GAN evaluation measures: New developments. *Computer Vision and Image Understanding* 215 (2022), 103329.
  - [22] Michael Boyle, Christopher Edwards, and Saul Greenberg. 2000. The effects of filtered video on awareness and privacy. In *Proceedings of the 2000 ACM conference on Computer supported cooperative work*. 1–10.
  - [23] Andrew Brock, Jeff Donahue, and Karen Simonyan. 2018. Large scale GAN training for high fidelity natural image synthesis. *arXiv preprint arXiv:1809.11096* (2018).
  - [24] Eoin Brophy, José Juan Dominguez Veiga, Zhengwei Wang, Alan F Smeaton, and Tomas E Ward. 2018. An interpretable machine vision approach to human activity recognition using photoplethysmograph sensor data. *arXiv preprint arXiv:1812.00668* (2018).
  - [25] Andreas Bulling, Ulf Blanke, and Bernt Schiele. 2014. A tutorial on human activity recognition using body-worn inertial sensors. *ACM Computing Surveys (CSUR)* 46, 3 (2014), 1–33.
  - [26] Eric Calais, Dominique Boisson, Steeve Symithe, Roberte Momplaisir, Claude Prépetit, Sophia Ulysse, Guy Philippe Etienne, Françoise Courboux, Anne Deschamps, Tony Monfret, et al. 2019. Can a Raspberry Shake seismic network complement a national seismic network? A case study in Haiti. (2019).
  - [27] Xi Hang Cao, Zoran Obradovic, and Kyungnam Kim. 2018. A Simple yet Effective Model for Zero-Shot Learning. *2018 IEEE Winter Conference on Applications of Computer Vision (WACV)* (2018), 766–774.
  - [28] Beichen Chen, Zhong Fan, and Fengming Cao. 2015. Activity recognition based on streaming sensor data for assisted living in smart homes. In *2015 International Conference on Intelligent Environments*. IEEE, 124–127.
  - [29] Liming Chen, Jesse Hoey, Chris D Nugent, Diane J Cook, and Zhiwen Yu. 2012. Sensor-based activity recognition. *IEEE Transactions on Systems, Man, and Cybernetics, Part C (Applications and Reviews)* 42, 6 (2012), 790–808.
  - [30] Lu Chi, Borui Jiang, and Yadong Mu. 2020. Fast fourier convolution. *Advances in Neural Information Processing Systems* 33 (2020), 4479–4488.
  - [31] Junyoung Chung, Caglar Gulcehre, KyungHyun Cho, and Yoshua Bengio. 2014. Empirical evaluation of gated recurrent neural networks on sequence modeling. *arXiv preprint arXiv:1412.3555* (2014).
  - [32] Aidan Clark, Jeff Donahue, and Karen Simonyan. 2019. Adversarial video generation on complex datasets. *arXiv preprint arXiv:1907.06571* (2019).
  - [33] Brian Clarkson, Kenji Mase, and Alex Pentland. 2000. Recognizing user context via wearable sensors. In *Digest of papers. Fourth international symposium on wearable computers*. IEEE, 69–75.
  - [34] CNET. 2023. Matter Smart Home Devices Dominated CES This Year. <https://www.cnet.com/home/smart-home/matter-smart-home-devices-dominated-ces-this-year/>
  - [35] Diane J Cook, Aaron S Crandall, Brian L Thomas, and Narayanan C Krishnan. 2012. CASAS: A smart home in a box. *Computer* 46, 7 (2012), 62–69.
  - [36] Pat Croskerry, Karen Cosby, Mark L Graber, and Hardeep Singh. 2017. *Diagnosis: Interpreting the shadows*. CRC Press.

- [37] Scott Davis and Carl Gutwin. 2005. Using relationship to control disclosure in Awareness servers.. In *Graphics Interface*, Vol. 5. Citeseer, 75–84.
- [38] Stephen Dawson-Haggerty, Andrew Krioukov, Jay Taneja, Sagar Karandikar, Gabe Fierro, Nikita Kitaev, and David Culler. 2013. {BOSS}: Building operating system services. In *10th USENIX Symposium on Networked Systems Design and Implementation (NSDI 13)*. 443–457.
- [39] Prafulla Dhariwal and Alexander Nichol. 2021. Diffusion models beat gans on image synthesis. *Advances in Neural Information Processing Systems* 34 (2021), 8780–8794.
- [40] Mengnan Du, Ninghao Liu, and Xia Hu. 2019. Techniques for interpretable machine learning. *Commun. ACM* 63, 1 (2019), 68–77.
- [41] Ali Erol, George Bebis, Mircea Nicolescu, Richard D Boyle, and Xander Twombly. 2007. Vision-based hand pose estimation: A review. *Computer Vision and Image Understanding* 108, 1-2 (2007), 52–73.
- [42] Jerry Fails and Dan Olsen. 2003. A design tool for camera-based interaction. In *Proceedings of the SIGCHI conference on Human factors in computing systems*. 449–456.
- [43] Giovanni Fusco, Ender Tekin, Richard E Ladner, and James M Coughlan. 2014. Using computer vision to access appliance displays. In *Proceedings of the 16th international ACM SIGACCESS conference on Computers & accessibility*. 281–282.
- [44] Wenbin Gao, Lei Zhang, Wenbo Huang, Fuhong Min, Jun He, and Aiguo Song. 2021. Deep neural networks for sensor-based human activity recognition using selective kernel convolution. *IEEE Transactions on Instrumentation and Measurement* 70 (2021), 1–13.
- [45] Munkhjargal Gochoo, Tan-Hsu Tan, Shih-Chia Huang, Shing-Hong Liu, and Fady S Alnajjar. 2017. DCNN-based elderly activity recognition using binary sensors. In *2017 international conference on electrical and computing technologies and applications (ICECTA)*. IEEE, 1–5.
- [46] Arieh Gomolin, Elena Netchiporouk, Robert Gniadecki, and Ivan V Litvinov. 2020. Artificial intelligence applications in dermatology: where do we stand? *Frontiers in medicine* 7 (2020), 100.
- [47] Ian Goodfellow, Jean Pouget-Abadie, Mehdi Mirza, Bing Xu, David Warde-Farley, Sherjil Ozair, Aaron Courville, and Yoshua Bengio. 2020. Generative adversarial networks. *Commun. ACM* 63, 11 (2020), 139–144.
- [48] Fuqiang Gu, Mu-Huan Chung, Mark Chignell, Shahrokh Valaee, Baoding Zhou, and Xue Liu. 2021. A Survey on Deep Learning for Human Activity Recognition. *ACM Comput. Surv.* 54, 8, Article 177 (oct 2021), 34 pages. <https://doi.org/10.1145/3472290>
- [49] Anhong Guo, Xiang'Anthony' Chen, Haoran Qi, Samuel White, Suman Ghosh, Chieko Asakawa, and Jeffrey P Bigham. 2016. Vizlens: A robust and interactive screen reader for interfaces in the real world. In *Proceedings of the 29th annual symposium on user interface software and technology*. 651–664.
- [50] Carl Erick Hagmann and Mary C Potter. 2016. Ultrafast scene detection and recognition with limited visual information. *Visual cognition* 24, 1 (2016), 2–14.
- [51] Olaf Hauk, Matthew H Davis, M Ford, Friedemann Pulvermüller, and William D Marslen-Wilson. 2006. The time course of visual word recognition as revealed by linear regression analysis of ERP data. *Neuroimage* 30, 4 (2006), 1383–1400.
- [52] Jonathan Ho, William Chan, Chitwan Saharia, Jay Whang, Ruiqi Gao, Alexey Gritsenko, Diederik P Kingma, Ben Poole, Mohammad Norouzi, David J Fleet, et al. 2022. Imagen video: High definition video generation with diffusion models. *arXiv preprint arXiv:2210.02303* (2022).
- [53] Jonathan Ho, Tim Salimans, Alexey Gritsenko, William Chan, Mohammad Norouzi, and David J Fleet. 2022. Video diffusion models. *Advances in Neural Information Processing Systems* (2022).
- [54] Sepp Hochreiter and Jürgen Schmidhuber. 1997. Long short-term memory. *Neural computation* 9, 8 (1997), 1735–1780.
- [55] Joanna M Holmgren and Maximilian J Werner. 2021. Raspberry Shake Instruments Provide Initial Ground-Motion Assessment of the Induced Seismicity at the United Downs Deep Geothermal Power Project in Cornwall, United Kingdom. *The Seismic Record* 1, 1 (2021), 27–34.
- [56] Weiming Hu, Tieniu Tan, Liang Wang, and Steve Maybank. 2004. A survey on visual surveillance of object motion and behaviors. *IEEE Transactions on Systems, Man, and Cybernetics, Part C (Applications and Reviews)* 34, 3 (2004), 334–352.
- [57] Scott E Hudson and Ian Smith. 1996. Techniques for addressing fundamental privacy and disruption tradeoffs in awareness support systems. In *Proceedings of the 1996 ACM conference on Computer supported cooperative work*. 248–257.
- [58] Taeho Hur, Jaehun Bang, Thien Huynh-The, Jongwon Lee, Jee-In Kim, and Sungyoung Lee. 2018. Iss2Image: A novel signal-encoding technique for CNN-based human activity recognition. *Sensors* 18, 11 (2018), 3910.
- [59] Tâm Huynh, Mario Fritz, and Bernt Schiele. 2008. Discovery of activity patterns using topic models. In *Proceedings of the 10th international conference on Ubiquitous computing*. 10–19.
- [60] Tâm Huynh and Bernt Schiele. 2005. Analyzing features for activity recognition. In *Proceedings of the 2005 joint conference on Smart objects and ambient intelligence: innovative context-aware services: usages and technologies*. 159–163.
- [61] Sadegh Bafandeh Imandoust, Mohammad Bolandraftar, et al. 2013. Application of k-nearest neighbor (knn) approach for predicting economic events: Theoretical background. *International journal of engineering research and applications* 3, 5 (2013), 605–610.
- [62] V Jahmunah, Eddie Yin Kwee Ng, Ru-San Tan, Shu Lih Oh, and U Rajendra Acharya. 2022. Explainable detection of myocardial infarction using deep learning models with Grad-CAM technique on ECG signals. *Computers in Biology and Medicine* 146 (2022), 105550.

- [63] Jeya Vikranth Jeyakumar, Joseph Noor, Yu-Hsi Cheng, Luis Garcia, and Mani Srivastava. 2020. How can i explain this to you? an empirical study of deep neural network explanation methods. *Advances in Neural Information Processing Systems* 33 (2020), 4211–4222.
- [64] Jeya Vikranth Jeyakumar, Ankur Sarker, Luis Antonio Garcia, and Mani Srivastava. 2023. X-CHAR: A Concept-based Explainable Complex Human Activity Recognition Model. *Proceedings of the ACM on Interactive, Mobile, Wearable and Ubiquitous Technologies* 7, 1 (2023), 1–28.
- [65] Shengyi Jiang, Guansong Pang, Meiling Wu, and Limin Kuang. 2012. An improved K-nearest-neighbor algorithm for text categorization. *Expert Systems with Applications* 39, 1 (2012), 1503–1509.
- [66] M Humayun Kabir, M Robiul Hoque, Hyungyu Seo, and Sung-Hyun Yang. 2015. Machine learning based adaptive context-aware system for smart home environment. *International Journal of Smart Home* 9, 11 (2015), 55–62.
- [67] Tero Karras, Samuli Laine, Miika Aittala, Janne Hellsten, Jaakko Lehtinen, and Timo Aila. 2020. Analyzing and improving the image quality of stylegan. In *Proceedings of the IEEE/CVF conference on computer vision and pattern recognition*. 8110–8119.
- [68] Yukitoshi Kashimoto, Kyoji Hata, Hirohiko Suwa, Manato Fujimoto, Yutaka Arakawa, Takeya Shigezumi, Kunihiro Komiya, Kenta Konishi, and Keiichi Yasumoto. 2016. Low-cost and device-free activity recognition system with energy harvesting PIR and door sensors. In *Adjunct Proceedings of the 13th International Conference on Mobile and Ubiquitous Systems: Computing Networking and Services*. 6–11.
- [69] Jasmeet Kaur and Anil Kumar. 2021. Speech emotion recognition using CNN, k-NN, MLP and random forest. In *Computer Networks and Inventive Communication Technologies: Proceedings of Third ICCNCT 2020*. Springer, 499–509.
- [70] Maninder Kaur, Gurpreet Kaur, Pradip Kumar Sharma, Alireza Jolfaei, and Dhananjay Singh. 2020. Binary cuckoo search metaheuristic-based supercomputing framework for human behavior analysis in smart home. *The Journal of Supercomputing* 76, 4 (2020), 2479–2502.
- [71] Bulat Khaertdinov and Stylianos Asteriadis. 2023. Explaining, Analyzing, and Probing Representations of Self-Supervised Learning Models for Sensor-based Human Activity Recognition. *arXiv preprint arXiv:2304.07304* (2023).
- [72] Atieh R Khamesi, Eura Shin, and Simone Silvestri. 2020. Machine learning in the wild: The case of user-centered learning in cyber physical systems. In *2020 International Conference on COMmunication Systems & NETworkS (COMSNETS)*. IEEE, 275–281.
- [73] Aftab Khan, Nils Hammerla, Sebastian Mellor, and Thomas Plötz. 2016. Optimising sampling rates for accelerometer-based human activity recognition. *Pattern Recognition Letters* 73 (2016), 33–40.
- [74] Pieter-Jan Kindermans, Sara Hooker, Julius Adebayo, Maximilian Alber, Kristof T Schütt, Sven Dähne, Dumitru Erhan, and Been Kim. 2019. The (un) reliability of saliency methods. In *Explainable AI: Interpreting, Explaining and Visualizing Deep Learning*. Springer, 267–280.
- [75] Maximilian A Köhl, Kevin Baum, Markus Langer, Daniel Oster, Timo Speith, and Dimitri Bohlender. 2019. Explainability as a non-functional requirement. In *2019 IEEE 27th International Requirements Engineering Conference (RE)*. IEEE, 363–368.
- [76] Ali Köksal, Kenan E Ak, Ying Sun, Deepu Rajan, and Joo Hwee Lim. 2023. Controllable Video Generation with Text-based Instructions. *IEEE Transactions on Multimedia* (2023).
- [77] Samantha Krening, Brent Harrison, Karen M Feigh, Charles Lee Isbell, Mark Riedl, and Andrea Thomaz. 2016. Learning from explanations using sentiment and advice in RL. *IEEE Transactions on Cognitive and Developmental Systems* 9, 1 (2016), 44–55.
- [78] Kestutis Kveraga and Moshe Bar. 2014. *Scene vision: Making sense of what we see*. Mit Press.
- [79] Nicholas D Lane, Petko Georgiev, and Lorena Qendro. 2015. Deeppear: robust smartphone audio sensing in unconstrained acoustic environments using deep learning. In *Proceedings of the 2015 ACM international joint conference on pervasive and ubiquitous computing*. 283–294.
- [80] Markus Langer, Daniel Oster, Timo Speith, Holger Hermanns, Lena Kästner, Eva Schmidt, Andreas Sesing, and Kevin Baum. 2021. What do we want from Explainable Artificial Intelligence (XAI)?—A stakeholder perspective on XAI and a conceptual model guiding interdisciplinary XAI research. *Artificial Intelligence* 296 (2021), 103473.
- [81] Gierad Laput, Yang Zhang, and Chris Harrison. 2017. Synthetic sensors: Towards general-purpose sensing. In *Proceedings of the 2017 CHI Conference on Human Factors in Computing Systems*. 3986–3999.
- [82] Oscar D Lara and Miguel A Labrador. 2012. A survey on human activity recognition using wearable sensors. *IEEE communications surveys & tutorials* 15, 3 (2012), 1192–1209.
- [83] Xinyu Li, Yanyi Zhang, Ivan Marsic, Aleksandra Sarcevic, and Randall S Burd. 2016. Deep learning for rfid-based activity recognition. In *Proceedings of the 14th ACM Conference on Embedded Network Sensor Systems CD-ROM*. 164–175.
- [84] Jessica Lin, Eamonn Keogh, Stefano Lonardi, and Bill Chiu. 2003. A symbolic representation of time series, with implications for streaming algorithms. In *Proceedings of the 8th ACM SIGMOD workshop on Research issues in data mining and knowledge discovery*. 2–11.
- [85] Hong Lu, Jun Yang, Zhigang Liu, Nicholas D Lane, Tanzeem Choudhury, and Andrew T Campbell. 2010. The jigsaw continuous sensing engine for mobile phone applications. In *Proceedings of the 8th ACM conference on embedded networked sensor systems*. 71–84.
- [86] Limeng Lu, Chuanlin Zhang, Kai Cao, Tao Deng, and Qianqian Yang. 2022. A multichannel CNN-GRU model for human activity recognition. *IEEE Access* 10 (2022), 66797–66810.



- [87] Scott M Lundberg and Su-In Lee. 2017. A unified approach to interpreting model predictions. *Advances in neural information processing systems* 30 (2017).
- [88] Aravindh Mahendran and Andrea Vedaldi. 2015. Understanding deep image representations by inverting them. In *Proceedings of the IEEE conference on computer vision and pattern recognition*. 5188–5196.
- [89] Andrea Manconi, Velio Coviello, Maud Galletti, and Reto Seifert. 2018. Monitoring rockfalls with the Raspberry Shake. *Earth Surface Dynamics* 6, 4 (2018), 1219–1227.
- [90] Elman Mansimov, Emilio Parisotto, Jimmy Lei Ba, and Ruslan Salakhutdinov. 2015. Generating images from captions with attention. *arXiv preprint arXiv:1511.02793* (2015).
- [91] M Martinez-Burdalo, A Martin, M Anguiano, and R Villar. 2004. Comparison of FDTD-calculated specific absorption rate in adults and children when using a mobile phone at 900 and 1800 MHz. *Physics in Medicine & Biology* 49, 2 (2004), 345.
- [92] Larry R Medsker and LC Jain. 2001. Recurrent neural networks. *Design and Applications* 5 (2001), 64–67.
- [93] Homay Danaei Mehr and Huseyin Polat. 2019. Human Activity Recognition in Smart Home With Deep Learning Approach. In *2019 7th International Istanbul Smart Grids and Cities Congress and Fair (ICSG)*. 149–153. <https://doi.org/10.1109/SGCF.2019.8782290>
- [94] Sakorn Mekruksavanich and Anuchit Jitpattanakul. 2021. Lstm networks using smartphone data for sensor-based human activity recognition in smart homes. *Sensors* 21, 5 (2021), 1636.
- [95] Tomas Mikolov, Ilya Sutskever, Kai Chen, Greg S Corrado, and Jeff Dean. 2013. Distributed representations of words and phrases and their compositionality. *Advances in neural information processing systems* 26 (2013).
- [96] Carina Mood. 2010. Logistic regression: Why we cannot do what we think we can do, and what we can do about it. *European sociological review* 26, 1 (2010), 67–82.
- [97] Tim Morris, Paul Blenkhorn, Luke Crossey, Quang Ngo, Martin Ross, David Werner, and Christina Wong. 2006. Clearspeech: A display reader for the visually handicapped. *IEEE Transactions on Neural Systems and Rehabilitation Engineering* 14, 4 (2006), 492–500.
- [98] David Murray, Lina Stankovic, and Vladimir Stankovic. 2021. Transparent AI: Explainability of deep learning based load disaggregation. In *Proceedings of the 8th ACM International Conference on Systems for Energy-Efficient Buildings, Cities, and Transportation*. 268–271.
- [99] Maryam M Najafabadi, Flavio Villanustre, Taghi M Khoshgoftaar, Naeem Seliya, Randall Wald, and Edin Muharemagic. 2015. Deep learning applications and challenges in big data analytics. *Journal of big data* 2, 1 (2015), 1–21.
- [100] Anzah H Niazi, Delaram Yazdarsepas, Jennifer L Gay, Frederick W Maier, Lakshmi Ramaswamy, Khaled Rasheed, and Matthew P Buman. 2017. Statistical Analysis of Window Sizes and Sampling Rates in Human Activity Recognition. In *HEALTHINF*. 319–325.
- [101] Norzaidah Md Noh, Azlin Ahmad, Shamimi Ab Halim, and Azliza Mohd Ali. 2012. Intelligent tutoring system using rule-based and case-based: a comparison. *Procedia-Social and Behavioral Sciences* 67 (2012), 454–463.
- [102] openAI. 2022. VDALL-E 2 is a new AI system that can create realistic images and art from a description in natural language. <https://openai.com/dall-e-2/>
- [103] Andrés Páez. 2019. The pragmatic turn in explainable artificial intelligence (XAI). *Minds and Machines* 29, 3 (2019), 441–459.
- [104] Trishan Panch, Heather Mattie, and Leo Anthony Celi. 2019. The “inconvenient truth” about AI in healthcare. *NPJ digital medicine* 2, 1 (2019), 77.
- [105] Vladimir I Pavlovic, Rajeev Sharma, and Thomas S. Huang. 1997. Visual interpretation of hand gestures for human-computer interaction: A review. *IEEE Transactions on pattern analysis and machine intelligence* 19, 7 (1997), 677–695.
- [106] Otávio AB Penatti and Milton FS Santos. 2017. Human activity recognition from mobile inertial sensors using recurrence plots. *arXiv preprint arXiv:1712.01429* (2017).
- [107] Thomas Plötz, Nils Y Hammerla, and Patrick L Olivier. 2011. Feature learning for activity recognition in ubiquitous computing. In *Twenty-second international joint conference on artificial intelligence*.
- [108] Samira Pouyanfar, Saad Sadiq, Yilin Yan, Haiman Tian, Yudong Tao, Maria Presa Reyes, Mei-Ling Shyu, Shu-Ching Chen, and Sundaraja S Iyengar. 2018. A survey on deep learning: Algorithms, techniques, and applications. *ACM Computing Surveys (CSUR)* 51, 5 (2018), 1–36.
- [109] MD Rakshith, H Harish, and GS Thyagaraju. 2017. A Smart Home Application for Resident Activity Prediction. *Journal of Android and IOS Applications and Testing* 2, 2 (2017).
- [110] Aditya Ramesh, Mikhail Pavlov, Gabriel Goh, Scott Gray, Chelsea Voss, Alec Radford, Mark Chen, and Ilya Sutskever. 2021. Zero-shot text-to-image generation. In *International Conference on Machine Learning*. PMLR, 8821–8831.
- [111] raspberry shake. 2022. As the world quieted down in 2020, Raspberry Shakes listened. <https://arstechnica.com/science/2020/12/as-the-world-quieted-down-in-2020-raspberry-shakes-listened/>
- [112] raspberry shake. 2022. raspberry shake home monitor. <https://raspberrysshake.org/>
- [113] Daniele Ravi, Charence Wong, Benny Lo, and Guang-Zhong Yang. 2016. A deep learning approach to on-node sensor data analytics for mobile or wearable devices. *IEEE journal of biomedical and health informatics* 21, 1 (2016), 56–64.
- [114] Vijay Ravindran, Ramprakash Ponraj, C Krishnakumar, Satheesh Ragnathan, V Ramkumar, and K Swaminathan. 2021. IoT-Based Smart Transformer Monitoring System with Raspberry Pi. In *2021 Innovations in Power and Advanced Computing Technologies (i-PACT)*. IEEE, 1–7.

- [115] Samir A Rawashdeh, Derek A Rafeldt, and Timothy L Uhl. 2016. Wearable IMU for shoulder injury prevention in overhead sports. *Sensors* 16, 11 (2016), 1847.
- [116] Ali Razavi, Aaron Van den Oord, and Oriol Vinyals. 2019. Generating diverse high-fidelity images with vq-vae-2. *Advances in neural information processing systems* 32 (2019).
- [117] Scott E Reed, Zeynep Akata, Santosh Mohan, Samuel Tenka, Bernt Schiele, and Honglak Lee. 2016. Learning what and where to draw. *Advances in neural information processing systems* 29 (2016).
- [118] Attila Reiss and Didier Stricker. 2012. Introducing a new benchmarked dataset for activity monitoring. In *2012 16th international symposium on wearable computers*. IEEE, 108–109.
- [119] Marco Tulio Ribeiro, Sameer Singh, and Carlos Guestrin. 2016. "Why should i trust you?" Explaining the predictions of any classifier. In *Proceedings of the 22nd ACM SIGKDD international conference on knowledge discovery and data mining*. 1135–1144.
- [120] Vincent Riquebourg, David Menga, David Durand, Bruno Marhic, Laurent Delahoche, and Christophe Loge. 2006. The smart home concept: our immediate future. In *2006 1st IEEE international conference on e-learning in industrial electronics*. IEEE, 23–28.
- [121] Mutegeki Ronald, Alwin Poulouse, and Dong Seog Han. 2021. iSPLInception: an inception-ResNet deep learning architecture for human activity recognition. *IEEE Access* 9 (2021), 68985–69001.
- [122] Phurich Saengthong and Seksan Laitrakun. 2021. Fusion Approaches of Heterogeneous Multichannel CNN and LSTM Models for Human Activity Recognition using Wearable Sensors. In *2021 13th International Conference on Information Technology and Electrical Engineering (ICITEE)*. IEEE, 183–188.
- [123] Andrea Rosales Sanabria, Franco Zambonelli, and Juan Ye. 2021. Unsupervised domain adaptation in activity recognition: A GAN-based approach. *IEEE Access* 9 (2021), 19421–19438.
- [124] Ramprasaath R Selvaraju, Michael Cogswell, Abhishek Das, Ramakrishna Vedantam, Devi Parikh, and Dhruv Batra. 2017. Grad-cam: Visual explanations from deep networks via gradient-based localization. In *Proceedings of the IEEE international conference on computer vision*. 618–626.
- [125] Ran Shao and Xiao-Jun Bi. 2022. Transformers Meet Small Datasets. *IEEE Access* 10 (2022), 118454–118464.
- [126] Donghee Shin. 2021. The effects of explainability and causability on perception, trust, and acceptance: Implications for explainable AI. *International Journal of Human-Computer Studies* 146 (2021), 102551.
- [127] Timo Speith. 2022. A review of taxonomies of explainable artificial intelligence (XAI) methods. In *2022 ACM Conference on Fairness, Accountability, and Transparency*. 2239–2250.
- [128] Chen Sun, Abhinav Shrivastava, Saurabh Singh, and Abhinav Gupta. 2017. Revisiting unreasonable effectiveness of data in deep learning era. In *Proceedings of the IEEE international conference on computer vision*. 843–852.
- [129] Ioan Susnea, Luminita Dumitriu, Mihai Talmaciu, Emilia Pecheanu, and Dan Munteanu. 2019. Unobtrusive monitoring the daily activity routine of elderly people living alone, with low-cost binary sensors. *Sensors* 19, 10 (2019), 2264.
- [130] Roman Suvorov, Elizaveta Logacheva, Anton Mashikhin, Anastasia Remizova, Arsenii Ashukha, Aleksei Silvestrov, Naejin Kong, Harshith Goka, Kiwoong Park, and Victor Lempitsky. 2022. Resolution-robust large mask inpainting with fourier convolutions. In *Proceedings of the IEEE/CVF Winter Conference on Applications of Computer Vision*. 2149–2159.
- [131] Tan-Hsu Tan, Munkhjargal Gochoo, Shih-Chia Huang, Yi-Hung Liu, Shing-Hong Liu, and Yun-Fa Huang. 2018. Multi-resident activity recognition in a smart home using RGB activity image and DCNN. *IEEE Sensors Journal* 18, 23 (2018), 9718–9727.
- [132] Emmanuel Munguia Tapia, Stephen S Intille, and Kent Larson. 2004. Activity recognition in the home using simple and ubiquitous sensors. In *International conference on pervasive computing*. Springer, 158–175.
- [133] Marco Taruselli, Diego Arosio, Laura Longoni, Monica Papini, and Luigi Zanzi. 2019. Raspberry shake sensor field tests for unstable rock monitoring. In *1st Conference on Geophysics for Infrastructure Planning Monitoring and BIM*, Vol. 2019. European Association of Geoscientists & Engineers, 1–5.
- [134] Ilya O Tolstikhin, Neil Houlsby, Alexander Kolesnikov, Lucas Beyer, Xiaohua Zhai, Thomas Unterthiner, Jessica Yung, Andreas Steiner, Daniel Keysers, Jakob Uszkoreit, et al. 2021. Mlp-mixer: An all-mlp architecture for vision. *Advances in neural information processing systems* 34 (2021), 24261–24272.
- [135] Tim Van Kasteren, Athanasios Noulas, Gwenn Englebienne, and Ben Kröse. 2008. Accurate activity recognition in a home setting. In *Proceedings of the 10th international conference on Ubiquitous computing*. 1–9.
- [136] Ashish Vaswani, Noam Shazeer, Niki Parmar, Jakob Uszkoreit, Llion Jones, Aidan N Gomez, Łukasz Kaiser, and Illia Polosukhin. 2017. Attention is all you need. *Advances in neural information processing systems* 30 (2017).
- [137] Jindong Wang, Yiqiang Chen, Shuji Hao, Xiaohui Peng, and Lisha Hu. 2019. Deep learning for sensor-based activity recognition: A survey. *Pattern recognition letters* 119 (2019), 3–11.
- [138] Kate Winter, Denis Lombardi, Alejandro Diaz-Moreno, and Rupert Bainbridge. 2021. Monitoring icequakes in East Antarctica with the raspberry shake. *Seismological Research Letters* 92, 5 (2021), 2736–2747.
- [139] Christine T Wolf. 2019. Explainability scenarios: towards scenario-based XAI design. In *Proceedings of the 24th International Conference on Intelligent User Interfaces*. 252–257.

- [140] Jason Wu, Chris Harrison, Jeffrey P. Bigham, and Gierad Laput. 2020. Automated Class Discovery and One-Shot Interactions for Acoustic Activity Recognition. In *Proceedings of the 2020 CHI Conference on Human Factors in Computing Systems* (Honolulu, HI, USA) (*CHI '20*). Association for Computing Machinery, New York, NY, USA, 1–14. <https://doi.org/10.1145/3313831.3376875>
- [141] Shuo Xiao, Shengzhi Wang, Zhenzhen Huang, Yu Wang, and Haifeng Jiang. 2022. Two-stream transformer network for sensor-based human activity recognition. *Neurocomputing* 512 (2022), 253–268.
- [142] Chao Xu, Shaoting Zhu, Junwei Zhu, Tianxin Huang, Jiangning Zhang, Ying Tai, and Yong Liu. 2023. Multimodal-driven Talking Face Generation, Face Swapping, Diffusion Model. *arXiv preprint arXiv:2305.02594* (2023).
- [143] Surong Yan, Yixing Liao, Xiaoqing Feng, and Yanan Liu. 2016. Real time activity recognition on streaming sensor data for smart environments. In *2016 International Conference on Progress in Informatics and Computing (PIC)*. IEEE, 51–55.
- [144] Xuzhong Yan, Heng Li, Angus R Li, and Hong Zhang. 2017. Wearable IMU-based real-time motion warning system for construction workers' musculoskeletal disorders prevention. *Automation in construction* 74 (2017), 2–11.
- [145] Wenyi Zhao, Rama Chellappa, P Jonathon Phillips, and Azriel Rosenfeld. 2003. Face recognition: A literature survey. *ACM computing surveys (CSUR)* 35, 4 (2003), 399–458.
- [146] Xiaochen Zheng, Meiqing Wang, and Joaquín Ordieres-Meré. 2018. Comparison of data preprocessing approaches for applying deep learning to human activity recognition in the context of industry 4.0. *Sensors* 18, 7 (2018), 2146.
- [147] Ian Zhou, Imran Makhdoom, Negin Shariati, Muhammad Ahmad Raza, Rasool Keshavarz, Justin Lipman, Mehran Abolhasan, and Abbas Jamalipour. 2021. Internet of things 2.0: Concepts, applications, and future directions. *IEEE Access* 9 (2021), 70961–71012.